International Geology Review, 2014
http://dx.doi.org/10.1080/00206814.2014.924037

Did the Turonian–Coniacian plume pulse trigger subduction initiation in the Northern Caribbean? Constraints from $^{40}Ar/^{39}Ar$ dating of the Moa-Baracoa metamorphic sole (eastern Cuba)

C. Lázaro[a]*, A. García-Casco[a,b], I.F. Blanco-Quintero[a,c], Y. Rojas-Agramonte[d,e], M. Corsini[f] and J.A. Proenza[g]

[a]*Departamento de Mineralogía y Petrología, Universidad de Granada, Granada, Spain;* [b]*Instituto Andaluz de Ciencias de la Tierra, CSIC-Universidad de Granada, Granada, Spain;* [c]*Departamento de Geociencias, Universidad de los Andes, Bogotá, Colombia;* [d]*Institut für Geowissenschaften, Universität Mainz, Mainz, Germany;* [e]*Departamento de Ciencias de la Tierra y de la Construcción, Universidad de las Fuerzas Armadas ESPE, Sangolquì, Ecuador;* [f]*Géosciences Azur UMR CNRS 6526, université de Nice Sophia-Antipolis, Nice cedex 02, France;* [g]*Departament Cristal·lografia, Mineralogia i Dipòsits Minerals, Universitat de Barcelona, Barcelona, Spain*

(*Received 7 April 2014; accepted 10 May 2014*)

The Güira de Jauco metamorphic sole, below the Moa-Baracoa ophiolite (eastern Cuba), contains strongly deformed amphibolites formed at peak metamorphic conditions of 650–660°C, approximately 8.6 kbar (~30 km depth). The geochemistry, based on immobile elements of the amphibolites, suggests oceanic lithosphere protholiths with a variable subduction component in a supra-subduction zone environment. The geochemical similarity and tectonic relations among the amphibolites and the basic rocks from the overlying ophiolite suggest a similar origin and protholith. New hornblende $^{40}Ar/^{39}Ar$ cooling ages of 77–81 Ma obtained for the amphibolites agree with this hypothesis, and indicate formation and cooling/exhumation of the sole in Late Cretaceous times. The cooling ages, geochemical evidence for a back-arc setting of formation of the mafic protoliths, and regional geology of the region allow proposal of the inception of a new SW-dipping subduction zone in the back-arc region of the northern Caribbean arc during the Late Cretaceous (ca. 90–85 Ma). Subduction inception was almost synchronous with the main plume pulse of the Caribbean–Colombian Oceanic Plateau (92–88 Ma) and occurred around 15 million years before arc-continent collision (75 Ma–Eocene) at the northern leading edge of the Caribbean plate. This chronological framework suggests a plate reorganization process in the region triggered by the Caribbean–Colombian mantle plume.

Keywords: ophiolite; metamorphic sole; Ar/Ar; Cuba; Caribbean–Colombian Oceanic Plateau

Introduction

Large ophiolitic complexes formed in two lithospheric domains, the Proto-Caribbean and the Caribbean, occur in the Circum-Caribbean region (e.g. Lewis *et al.* 2006; Figure 1). The Proto-Caribbean (i.e. Atlantic-related) oceanic lithosphere formed between North and South America during the Late Jurassic–Cretaceous after the break up of Pangea. Oceanic lithosphere also forms the basement of the Pacific (Farallon)-derived Caribbean plate, which contains the Caribbean–Colombian Oceanic Plateau (CCOP; Figure 1) characterized by large volumes of tholeiitic basalts and minor picrites and komatiites (Kerr *et al.* 2003) formed during the Late Cretaceous (92–88 Ma; Sinton *et al.* 1998; Hastie and Kerr 2010, etc.). Different tectonic models have been proposed to explain the evolution of the Caribbean region. On the one hand, the volcanic arc of the Caribbean formed since the early Cretaceous (ca. 135 Ma) after the inception of a W-dipping subduction zone along a sinistral 'inter-American transform' that would connect the E-dipping subduction zones fringing the western margins of North and South America (Figure 1b; Pindell *et al.* 2012, and references therein). On the other hand, a Turonian–Campanian subduction polarity reversal, from E-dipping subduction of Farallon to W-dipping subduction of the Proto-Caribbean, occurred as a result of collision of the CCOP with the Caribbean arc (Figure 1d; Duncan and Hargraves 1984; Burke 1988; Kerr *et al.* 1999, 2003; Hastie *et al.* 2013). The two models agree in regard to W-dipping subduction of the Proto-Caribbean, but conflict in regard to the timing of subduction initiation (Early Cretaceous vs. Late Cretaceous). West-dipping subduction of the Proto-Caribbean caused subduction of the continental margins of North America and arc-continent collision in the northern leading edge of the Caribbean in the latest Cretaceous–earliest Tertiary (García-Casco *et al.* 2008a; Iturralde-Vinent *et al.* 2008; Solari *et al.* 2013, and references therein). During this event, ophiolitic complexes were obducted onto the continental margin in Guatemala, Cuba, and Hispaniola (Anderson *et al.* 1985; Pindell and Draper 1991; De Zoeten and Mann 1999; Pindell *et al.* 2005; Iturralde-Vinent *et al.* 2006).

*Corresponding author. Email: clazaro@ugr.es

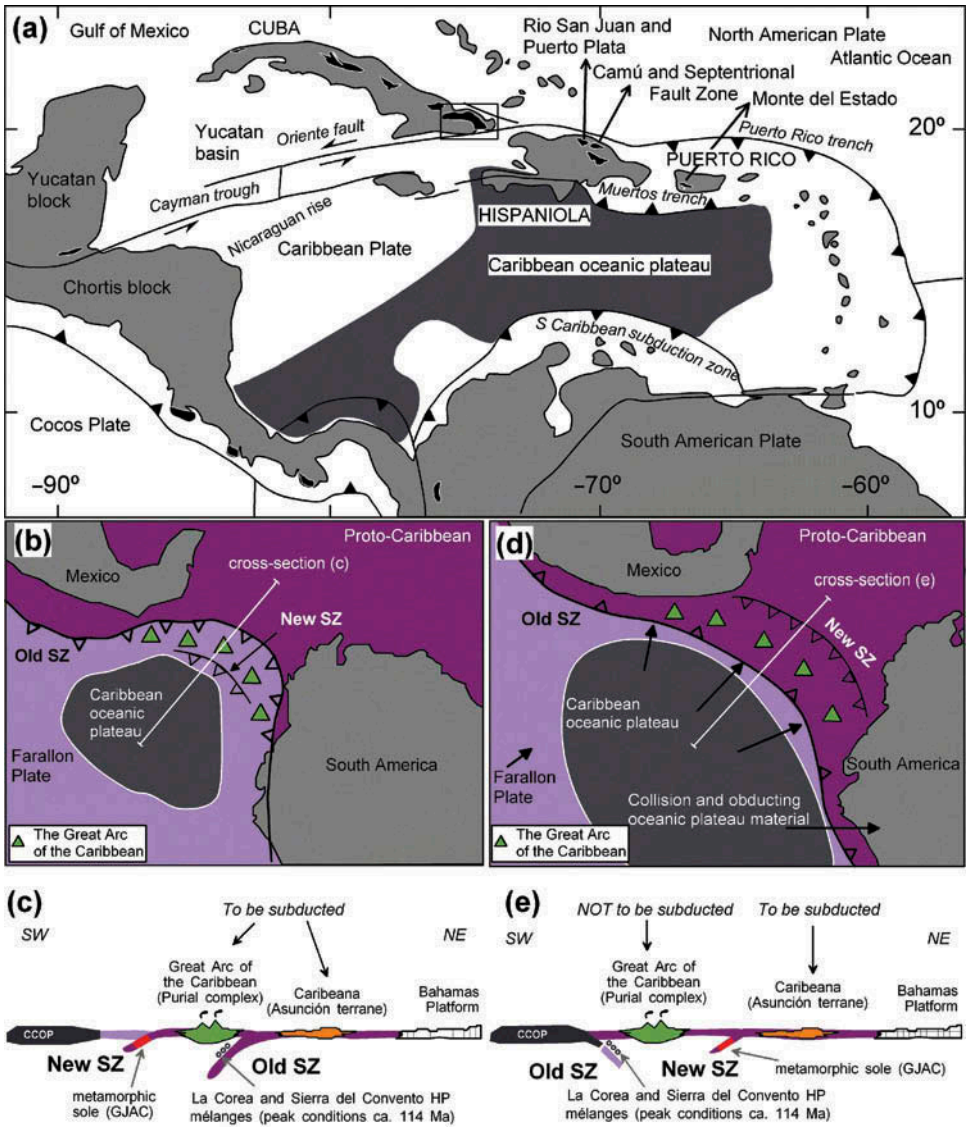

Figure 1. (a) Plate tectonic configuration of the Caribbean region; (b) model and (c) related SW–NE schematic cross-section for the Caribbean region at ca. 85 Ma based on Pindell and Kennan (2009), García-Casco *et al.* (2008a), Pindell *et al.* (2012), and Lázaro *et al.* (2013); (d) model and (e) related SW–NE schematic cross-section for the Caribbean region at ca. 85 Ma based on the oceanic plateau reversal model by Duncan and Hargraves (1984), Burke (1988), Kerr *et al.* (1999, 2003), and Hastie *et al.* (2013).

The Güira de Jauco Amphibolite Complex (GJAC, eastern Cuba; Figure 2) was recently proposed as a sub-ophiolitic metamorphic sole related to subduction inception of the Caribbean back-arc basin (Lázaro *et al.* 2013), and hence it is a key element for deciphering the evolution of Caribbean tectonics. The age of metamorphism is, however, imprecise (72 ± 3 and 58 ± 4 Ma, amphibole and whole-rock K–Ar, respectively; Somin and Millán 1981). The main focus of this paper is the Ar/Ar dating of the amphibolites and to discuss the geodynamic evolution of the NW segment of the Caribbean realm.

Geological setting

The Cuban fragment of the Caribbean orogenic belt formed during the Cretaceous–Tertiary convergence of the Caribbean oceanic plate and the North American margin (Iturralde-Vinent 1998). Cretaceous subduction of the Proto-Caribbean (i.e. Atlantic oceanic lithosphere formed during the break-off of Pangea and ensuing continental drifting) below the Caribbean plate formed an intra-oceanic arc system that finally collided with the Jurassic–Cretaceous passive margin-like terrane of Caribeana, the margin of the continental Maya block (Guaniguanico terrane), and the Bahamas platform in latest Cretaceous–

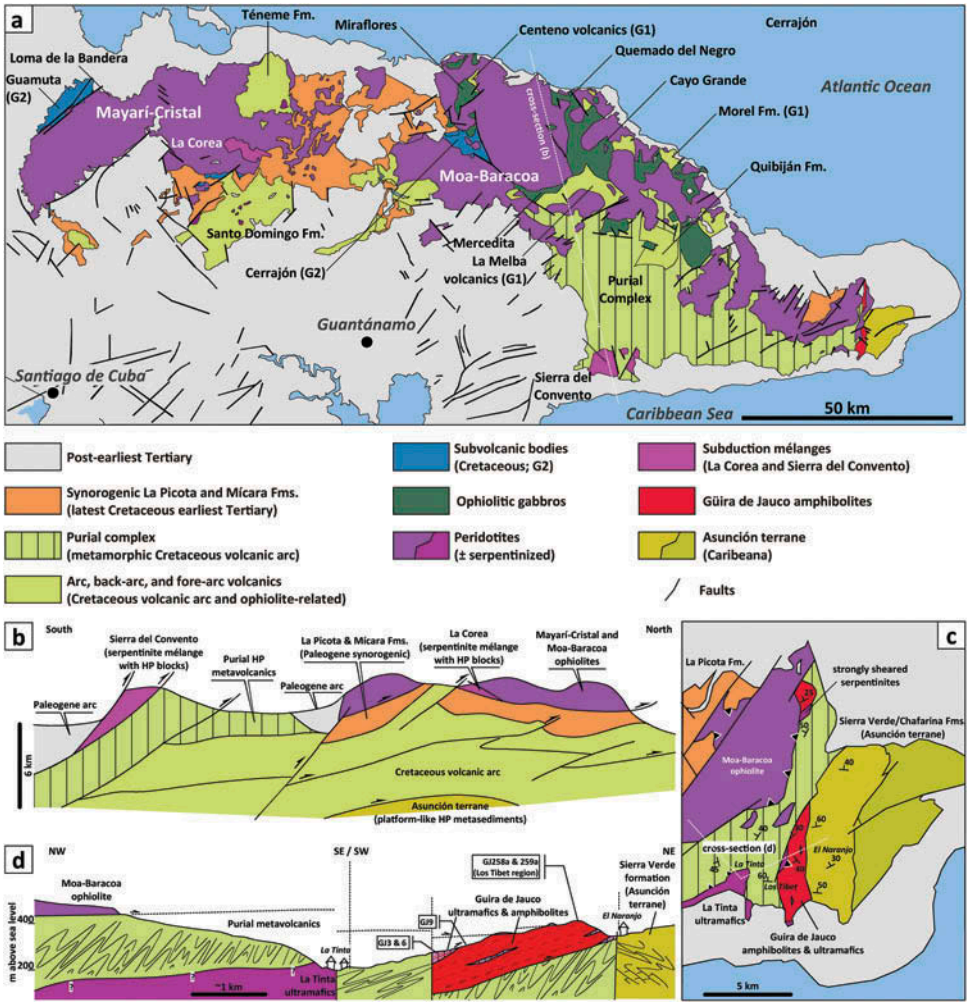

Figure 2. (a) Geological map of eastern Cuba showing the main geological units (Pushcharovsky 1988); (b) schematic cross-section of eastern Cuba (modified from Iturralde-Vinent 1998); (c) geological map of the Güira de Jauco Amphibolite Complex (based on the Geologic Map of the Republic of Cuba, scale 1:100, 000, sheet 5376, Instituto de Geología y Paleontología, La Habana) showing sample locations: GJ-3 (74º18′29″, 20º7′22″), GJ-6 (74º18′30.1″, 20º7′22.3″), GJ-9 (74º18′41.09″, 20º8′19.82″), GJ-258a (74º18′30.15″, 20º6′49.65″), and GJ-259a (74º18′36.9″, 20º6′54.27″); (d) cross-section of the Güira de Jauco Amphibolite Complex and adjacent complexes, as indicated in (c).

Tertiary times (García-Casco *et al.* 2008a; Iturralde-Vinent *et al.* 2008). The collision triggered the tectonic emplacement of several oceanic units (including volcanic arc, ophiolite, and subduction mélange units), as well as subducted and non-subducted continental margin rocks and syntectonic basin sequences, onto the margin of North America.

The geology of eastern Cuba includes several of these tectonic units (Figure 2a), namely ophiolitic bodies (i.e. the Mayarí-Cristal and Moa-Baracoa complexes), volcanic arc sequences (i.e. Purial, Quibiján, Santo Domingo, Téneme, and Morel formations), subduction mélanges (i.e. Sierra del Convento and La Corea), subducted metasedimentary rocks (i.e. Sierra Verde and Chafarina formations of the Asunción terrane), and synorogenic basins (i.e. La Picota and Mícara formations). The general vergence of the thrusting structures is towards the NE (Figure 2b; Cobiella *et al.* 1984; Nuñez Cambra *et al.* 2004). These directions are mostly related to the final (cold) emplacement of the ophiolitic and volcanic arc sheets during the latest Cretaceous and early Danian (Iturralde-Vinent *et al.* 2006). Below, we describe the main geological features of these complexes from top-down in the structural pile.

The most significant tectonic units in the area are the Cretaceous volcanic arc and the ophiolitic belts, which constitute, structurally, the highest pre-Tertiary complexes in the region. The huge Mayarí-Baracoa Ophiolitic belt (MBOB; Iturralde-Vinent 1996a; Proenza *et al.* 1999; Cobiella-Reguera 2005) is 170 km long, 10–30 km wide, and on average 3.5 km thick, but it consists, in fact, of two

main massifs (Figure 2a and b) probably emplaced as independent tectonic units: the Mayarí-Cristal Ophiolite Massif to the west and the Moa-Baracoa Ophiolite Massif to the east (Proenza *et al.* 1999). The Mayarí-Cristal Ophiolite Massif is made up of harzburgite tectonite hosting minor subconcordant dunite layers, chromitites, and subordinate discordant microgabbro and diabase dikes, probably formed in a back-arc environment, while the Moa-Baracoa Ophiolite Massif is mostly composed of highly depleted harzburgitic tectonites and dunites crosscut by gabbroic dikes (locally pegmatitic) overlain by impregnated peridotites with plagioclase, gabbroic sills, and cumulate gabbroic (approximately 500 m thick) rocks with a suprasubduction geochemical signature formed in a back-arc to arc environment (Proenza *et al.* 1999; Marchesi *et al.* 2006, 2007). Zircons from a gabbroic dike from Cayo Grande, northeast of Baracoa (Moa–Baracoa massif) have a $^{206}Pb/^{238}U$ age of ca. 124 Ma (Rojas-Agramonte *et al.* 2013), suggesting formation of the oceanic lithosphere since at least Early Cretaceous times. The thicknesses of the Mayarí-Cristal and Moa–Baracoa sheets are estimated at >5 and 2.2 km, respectively (Marchesi *et al.* 2006). The relative positions of the sheets in the structural pile have not been assessed.

Serpentinitic mélanges containing high-P blocks (Figure 2a and b) occur tectonically below the Mayarí–Cristal massif (La Corea mélange; Blanco-Quintero *et al.* 2010) and as a body disconnected from the main ophiolitic massifs (Sierra del Convento mélange; Garcia-Casco *et al.* 2008b). These mélanges contain exotic HP blocks of various origins, sizes, and compositions (Ep ± Grt-, Pl-lacking amphibolites, tonalitic-trondhjemitic rocks, blueschists, jadeitites) within a serpentinite matrix, which document subduction of oceanic lithosphere since at least 120 Ma (García-Casco *et al.* 2006; Lázaro and García-Casco 2008; 2008b, 2009; Lázaro *et al.* 2009; Blanco-Quintero *et al.* 2010, 2011a; Cárdenas-Párraga *et al.* 2012). The serpentinitic matrix is essentially composed of sheared serpentinite within massive antigoritite blocks (Blanco-Quintero *et al.* 2011b). The peak P-T conditions of the earliest subducted metamorphic blocks (Ep ± Grt, Pl-lacking amphibolites) attained 700–750ºC and ~1.5 GPa, above the wet solidus of basaltic rocks, and in fact represent residual rocks formed after partial melting and generation of tonalitic–trondhjemitic melts that crystallized *in situ* within the amphibolites at 1.5 GPa (García-Casco *et al.* 2006; Garcia-Casco 2007; Lázaro and García-Casco 2008; 2008b; Lázaro *et al.* 2009; Blanco-Quintero *et al.* 2010). SHRIMP U-Pb zircon dating of the tonalitic-trondhjemitic rocks yields ca. 115 Ma, indicating active subduction of oceanic crust at ca. 120 Ma, while Ar–Ar dating of hornblende and micas yields Late Cretaceous ages ranging 105–80 Ma, indicating slow exhumation in the subduction channel (Lázaro *et al.* 2009; Blanco-Quintero *et al.* 2011a). Associated jadeitites in the Sierra del Convento mélange formed at 1.5 GPa, approximately 550ºC, and yield U–Pb zircon SHRIMP ages of ca. 108 Ma (Cárdenas-Párraga *et al.* 2012). The amphibolitic blocks are of mid-ocean ridge basalt (MORB) composition and followed counterclockwise P-T paths, indicating onset of subduction of hot (very young) oceanic lithosphere at ca. 120 Ma. Other tectonic blocks within the mélanges are of blueschist facies rocks bearing glaucophane and lawsonite. Petrological, geochemical, and geochronologic data are not available, but they can be conceptualized as material subducted and accreted to the mélanges late in their evolution in the subduction channel, probably during the Late Cretaceous, as documented in the nearby Río San Juan mélange, Dominican Republic (Krebs *et al.* 2008, 2011; Escuder-Viruete *et al.* 2013).

The ophiolitic thrust sheets override syntectonic foredeep-related Maastrichtian–lower Danian olistostromal Mícara (Cobiella 1974) and La Picota (Lewis and Straczek 1955) formations (Figure 2a and b) (see also Iturralde-Vinent 1976; Cobiella *et al.* 1984; Quintas 1987). These formations occupy an intermediate discontinuous tectonic position below the ophiolite thrust sheets and the underlying volcanic arc formations (Iturralde-Vinent *et al.* 2006). Well-bedded, graded, polymictic sandstones (including centimetre-sized layers of serpentinitic sandstones and gravels) and shales, with local intercalations of conglomerates and breccias constitute the Mícara Formation (Fm.). The La Picota Fm. occurs above of, and as lenticular intercalations within, the Mícara Fm. It is formed by massive chaotic layers of large-grain-size (pebbles, blocks, and boulders) detrictic rocks of ultramafic rocks, serpentinites, and gabbroids with local fragments of the Mícara Fm. Both formations are strongly intermingled with olistoliths and olistoplates composed of mafic–ultramafic rocks and the volcanic arc-related Santo Domingo Fm. and Purial complex (Cobiella 1974; Iturralde-Vinent 1976; Quintas 1987; Iturralde-Vinent *et al.* 2006), indicating deposition in a deep basin facing the thrust front and final tectonic emplacement and sub-aerial exposure of the ophiolites and volcanic arc units in the latest Maastrichtian to early Danian (Iturralde-Vinent *et al.* 2006).

The ophiolite sheets, mélanges, and syntectonic sedimentary formations tectonically override Cretaceous volcanic units (e.g. Téneme, Santo Domingo, Purial, Quibiján, and Morel volcanic formations; Figure 2; Knipper and Cabrera 1974; Iturralde-Vinent 1976, 1996a, 1996b; Quintas 1988, 1989; Torrez and Fonseca 1990; Gyarmati *et al.* 1997; Kerr *et al.* 1999; Iturralde-Vinent *et al.* 2006). These units are mafic to felsic in composition and have distinct geochemical signatures (MORB-like, tholeiitic, boninitic, and calc-alkaline lavas) documenting axial-arc, back-arc, and fore-arc environments during Early (Aptian-Albian) to Late Cretaceous (mid-Campanian) times (Iturralde-Vinent *et al.* 2006; Proenza *et al.* 2006; Marchesi *et al.* 2007, and references therein).

The Morel, La Melba, and Centeno volcanics (Figure 2a; Group G1 of Marchesi *et al.* 2007) consist of tholeiitic basalts and rare basaltic andesites that have normal mid-ocean ridge basalt (N-MORB)-like compositions similar to those found in back-arc basin basalts. The Guamuta, Loma de la Bandera, and Cerrajón dike complexes (Figure 2a; Group G2 of Marchesi *et al.* 2007) comprise basaltic and rare basaltic andesitic subvolcanic dikes with major- and trace element and isotopic compositions similar to those of island arc tholeiites. The Téneme, characterized as varying between low-Ti island arc tholeiites (IAT) with boninitic affinity and typical oceanic arc tholeiites (Proenza *et al.* 2006) and calc-alkaline Quibiján volcanic arc formations (Figure 2a), has an unambiguous subduction-related character (Marchesi *et al.* 2007). On the other hand, Gyarmati *et al.* (1997) suggested a tholeiite and calc-alkaline affinity of the Santo Domingo volcanics based on major element geochemistry. The Purial complex is geochemically described as calc-alkaline (Millán 1996) or tholeiitic to calc-alkaline arc-related rocks (Gyarmati *et al.* 1997). Fragments of the Campanian and older Cretaceous volcanic arc of the Caribbean (the Purial complex) underwent high-P metamorphism, which developed strongly deformed lawsonite- and glaucophane-bearing blueschist facies rocks and high-pressure greenschists (Figure 2; Boiteau *et al.* 1972; Somin and Millán 1981; Cobiella *et al.* 1984; Millán *et al.* 1985). The age of subduction-related metamorphism is latest Cretaceous (ca. 75–70 Ma; Somin and Millán 1981; Somin *et al.* 1992; Iturralde-Vinent *et al.* 2006). In fact, the late Campanian demise of the Caribbean volcanic arc indicates a Late Cretaceous–earliest Tertiary collision-accretion event, when final obduction of the ophiolites occurred on top of the volcanic arc units (García-Casco *et al.* 2008a, and references therein).

Tectonic slices of ultramafic rocks are located tectonically within and below the volcanic arc formations, either metamorphosed (i.e. Purial complex) or not, as in the La Tinta area close to the studied region (Figure 2c and d). These ultramafic slices have not been studied in detail, but preliminary unpublished data suggest that in the La Tinta region the slice formed during the Early Cretaceous in a fore-arc environment.

García-Casco *et al.* (2008a) considered that the metasedimentary Asunción terrane is the lowest tectonic unit in the region (Figure 2b; see, however, Cobiella *et al.* 1984 for a different view) and related it to the Caribeana platform terrane of the Proto-Caribbean, which subducted during the latest Cretaceous–earliest Tertiary. The main contacts of this complex with other complexes are hidden by strong weathering, vegetation, and intense late steep faulting probably related to the late Eocene/early Oligocene to Present activity of the Oriente Transform fault system (Figure 1a) that dissects the Caribbean belt south of Cuba and separates the Cuban branch from the Caribbean plate (Rojas-Agramonte *et al.* 2006 and references therein). The Asunción terrane is made of two lithologic formations, the Chafarina and Sierra Verde Fms (Figure 2c; Somin and Millán 1972; Gyarmati 1983; Cobiella *et al.* 1984; Millán and Somin 1985; Millán *et al.* 1985; Millán 1997). The Chafarina Fm. is composed mainly of calcitic and dolomitic marbles, commonly bearing graphite (black marbles) with occasional micaceous material, that have been correlated with the Upper Jurassic and Cretaceous calcareous sections of the subducted Escambray (Central Cuba) or non-subducted Guaniguanico (Western Cuba) terranes (Millán and Somin 1985; Millán *et al.* 1985; Millán 1997) and with the isochronous sections of the non-subducted Remedios-Camajuaní belts of the Bahamas borderland (Central Cuba; Iturralde-Vinent 1998). The Sierra Verde Fm. is composed of impure quartzites and phyllites rich in graphite, with some intercalations of metabasalts, grey marbles, and metaradiolarites with depositional ages between the Tithonian and the Lower Cretaceous (Millán and Somin 1985, Millán *et al.* 1985). The metamorphic assemblages of the phyllites and the metabasaltic rocks of the Sierra Verde Fm. contain lawsonite and glaucophane (Millán 1997), indicating subduction-related HP/LT metamorphism. Detailed petrologic analysis, P-T estimations, and geochronologic determinations are lacking, but a pre-early Danian metamorphic age is suggested by Iturralde-Vinent *et al.* (2006) based on stratigraphic arguments, in agreement with regional considerations (i.e. as in the Samaná Complex, Dominican Republic; Escuder-Viruete *et al.* 2011).

The Güira de Jauco amphibolite complex

The Güira de Jauco Amphibolite Complex (GJAC) forms a thin strip roughly oriented N–S at the easternmost edge of the Moa–Baracoa Ophiolite Massif (Figure 2a and c). This amphibolitic strip has been interpreted as the metamorphic sole of the Moa–Baracoa ophiolite (Figure 3a; Lázaro *et al.* 2013). The amphibolites are of basaltic MORB-like protholith formed in a back-arc setting (Lázaro *et al.* 2013). These authors identified geochemical similarities to the latest Turonian–Coniacian (palaeontological age; Iturralde-Vinent *et al.* 2006) volcanic and plutonic rocks related to the Moa–Baracoa ophiolite formed in a back-arc setting (Marchesi *et al.* 2007). Concordant layers of marbles and quartzite locally occur within the amphibolites (Figure 3d). The latter rock type probably represents metachert, suggesting that the protoliths of the amphibolites are, at least in part, basalts deposited in a deep basin.

The main lithologies are garnet amphibolite, clinopyroxene amphibolite, and common amphibolite. The garnet amphibolites are mainly composed of calcic amphibole (of pargasite and ferropargasite composition; Lázaro *et al.*

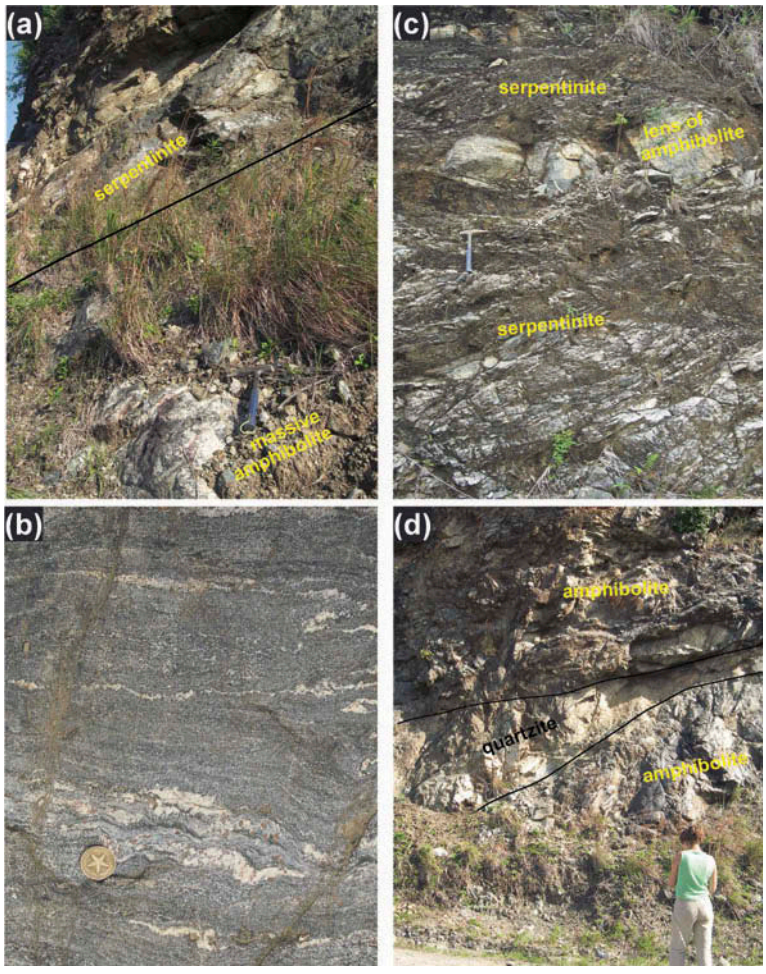

Figure 3. (a) Tectonic contact between serpentinites (above) and the main body of amphibolites (below); (b) amphibolite layer within serpentinites; (c) melt segregations in garnet amphibolites; (d) quartzite layer within amphibolites.

2013), plagioclase (oligoclase cores and andesine rims), epidote, and garnet. Accessory titanite, ± rutile, and ± quartz are also present. Amphibole, plagioclase, and epidote are oriented following the main foliation (Figure 4a). Frequently, the garnets display porfidoblastic texture and commonly have inclusion trails (rutile, titanite, epidote, calcic amphibole) oriented parallel to or at a small angle with the external foliation, indicating syn-kinematic growth. The clinopyroxene amphibolites are composed of calcic amphibole (edenite-Fe/Mg pargasite-magnesiohornblende, in rocks with higher TiO_2 contents, and magnesiohorblende-actinolite, in rocks with lower TiO_2 contents; see Lázaro *et al.* 2013 for details), plagioclase (andesine cores and albite rims), epidote, clinopyroxene (diopside; see Lázaro *et al.* 2013), and accessory titanite and retrograde chlorite. The differences in bulk compositions of these two types of samples (high- and low-Ti) are mirrored by amphibole compositions (Lázaro *et al.* 2013). Amphibole, plagioclase, and clinopyroxene are well oriented along the foliation (Figure 4b). The common amphibolites are mainly composed of amphibole (pargasite-edenite and tschermakite-magnesiohorblende), plagioclase (oligoclase cores and andesine rims), epidote (locally absent), and accessory titanite, with amphibole, epidote, and plagioclase stretched and oriented along the main foliation (Figure 4c and d). The marbles (Figure 4e) and quartzites (Figure 4f) display grain-size reduction and recrystallization textures. The quartzites are composed of quartz plus minor amounts of plagioclase and accessory epidote and calcic amphibole.

Locally, partial melting structures are apparent (Figure 3b), indicating peak metamorphic conditions above the wet basalt solidus. The calculated peak P-T conditions of garnet amphibolites, closely related to partial melts, and of clinopyroxene amphibolites, not spatially related to partial melts, are indistinguishable and just at the wet basaltic solidus, 650–665°C and 8.5–8.7 kbar (Lázaro *et al.* 2013), indicating that fluid infiltration and/or bulk-rock composition rather than metamorphic conditions locally triggered partial melting. These results and

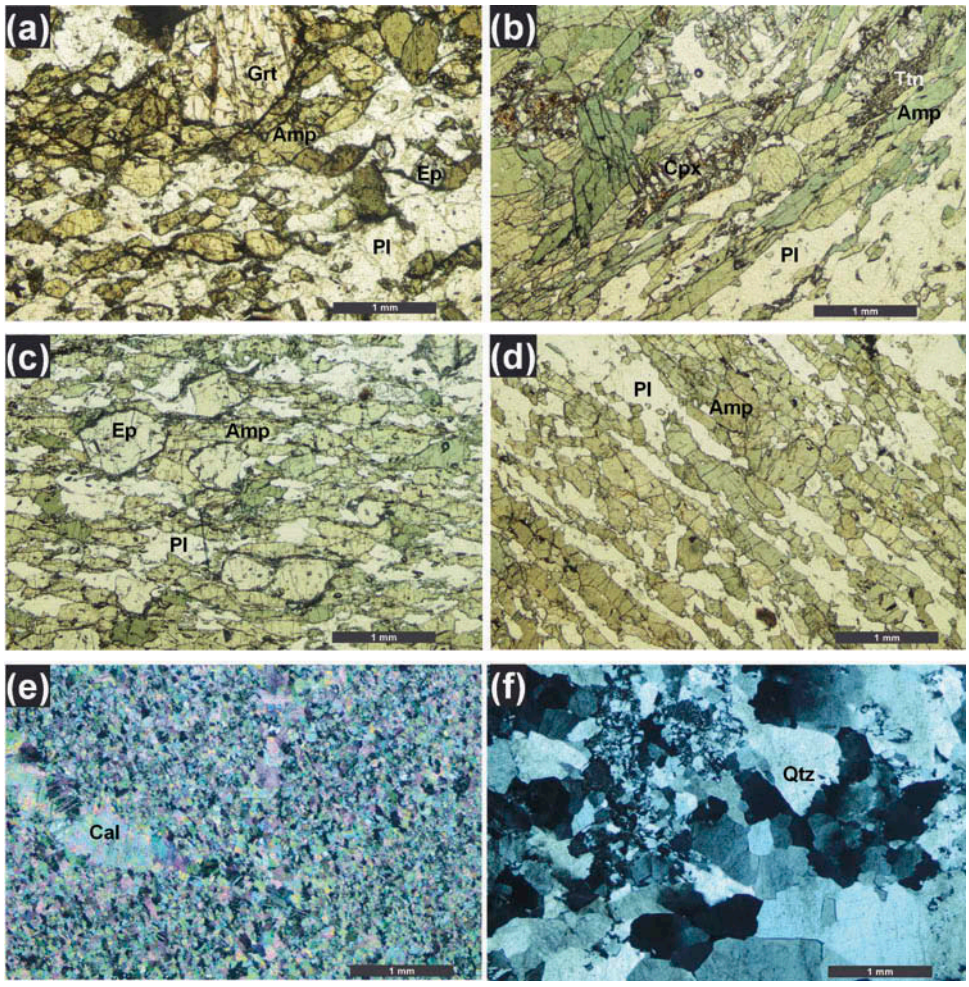

Figure 4. Photomicrographs of (a) garnet amphibolite, (b) clinopyroxene amphibolite, (c) epidote-bearing amphibolite, (d) amphibolite, (e) marble (crossed polars), and (f) quartzite (crossed polars). Abbreviations; Grt, garnet; Amp, amphibolite; Rt, rutile; Ep, epidote; Cpx, clinopyroxene; Pl, plagioclase; Ttn, titanite; Cal, calcite; Qtz, quartz.

the uniform amphibolite facies conditions in the main amphibolite body do not allow deciphering of the distribution of metamorphic zones, if present. In fact, the variability in mineral assemblage is not related to contrasted P-T conditions but to bulk-rock composition effects (Lázaro *et al.* 2013). However, it should be noted that the observed partial melting structures occur at the highest structural levels of the amphibolitic complex (approximately 400 m above sea level, close to the Los Tibet community; Figures 2c and 3b), suggesting (but not proving) an inverted metamorphic gradient.

Ultramafic slices (serpentinites s.s. and serpentinized harzburgites) less than a few tens of metres thick appear on top of, and within, the main body of amphibolites (Figure 2c and d). While some of the tectonic slices on top of the amphibolites represent fragments of the Moa–Baracoa ophiolitic serpentinized harzburgites, other slices of serpentinites (on top and within the body) contain co-facial centimetre- to metre-sized layers of epidote amphibolites and, less commonly, hornblendites and clinopyroxene amphibolites, concordant with the main foliation of the serpentinites (Figure 3c). The mineral assemblages of these amphibolite layers, composed of calcic amphibole (pargasite–edenite and tschermakite–magnesiohorblende), ± plagioclase (oligoclase cores), ± epidote, ± clinopyroxene (diopside), plus accessory titanite and/or rutile (Figure 5a), are similar to those of the main amphibolitic body. The hornblendites are composed almost exclusively of amphibole with accessory epidote (Figure 5b). In general the amphibolite layers display strong foliation and nematoblastic texture, though random disposition of amphibole in some samples indicates deformation partitioning with deformation focused in the enclosing serpentinites. The enclosing serpentinites are foliated and folded antigoritites (Figure 5c and d) bearing chlorite and magnetite and, locally, tremolite, plus olivine and orthopyroxene relicts (Figure 5e and f) partly replaced by chlorite, antigorite, and chrysotile (with mesh texture).

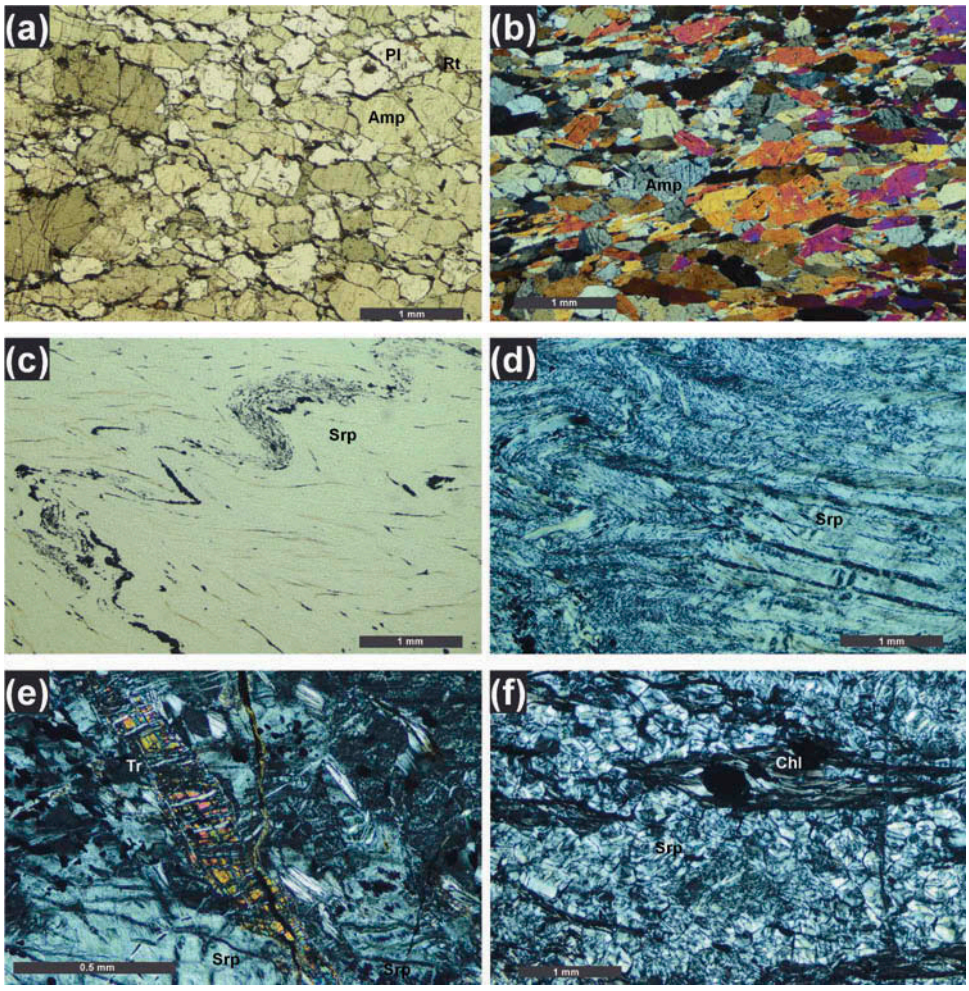

Figure 5. Photomicrographs of (a) epidote amphibolite layer within serpentinite, (b) hornblendite within serpentinite, (c) folded serpentinite, (d) highly deformed serpentinite (crossed polars), (e) tremolite in serpentinite (crossed polars), and (f) chlorite in serpentinite (crossed polars). Abbreviations: Srp, serpentine; Chl, chlorite; Rt, rutile; Amp, amphibole; Pl, plagioclase.

Tremolite-bearing assemblages probably formed as a function of whole-rock composition (Ca-richer metaperidotites) and are consistent with amphibolite facies conditions, in agreement with a common metamorphic history with the enclosed epidote-bearing amphibolite layers. We hence interpret that these serpentinites bearing amphibolite layers form part of the metamorphic sole rather than being slices of the non-metamorphic (except for low-T serpentinization) Moa–Baracoa ophiolite, though their position on top of and within the amphibolite body indicates tectonic relationships. As discussed below, we interpret that emplacement of the serpentinitic slices occurred during the initial exhumation of the metamorphic sole.

As indicated, the whole complex is highly deformed and locally mylonitic. The general dip of the foliation is moderate, about 40–20º towards the NW (Figure 2d). The attitude of the foliation is cut by the eastern and western contacts of the body with the meta-sediments of the Asunción terrane (Sierra Verde Fm.) and the Purial metavolcanics, respectively, indicating steep fault-bounded contacts probably related to the Tertiary activity of the Oriente Fault (Figure 1a). The general geologic relations, however, indicate that the amphibolitic body appears tectonically below the non-metamorphic ultramafic rocks of the Moa–Baracoa ophiolitic belt (Figure 3a) and above the metavolcanic Purial complex to the west (Figure 2d). The basal tectonic contact of the Moa–Baracoa ophiolite, however, cross-cuts both the Purial and Güira de Jauco complexes (Figure 2d), suggesting that the thrust contact is late and unrelated to the formation of the amphibolitic sole. The estimated thickness of the complex is approximately 200 m (perpendicular to the average main foliation; Figure 2d).

Sample description

Two garnet amphibolite samples (GJ-258a, GJ-259a) and one epidote-bearing common amphibolite (GJ-9) sample

Table 1. Representative analyses of amphibole (normalized to 22 O and 2 OH).

Sample	GJ9	GJ258a	GJ259a
SiO_2	46.99	41.97	41.65
TiO_2	0.480	0.767	0.767
Al_2O_3	10.21	14.72	15.64
FeO	10.81	15.40	14.38
MnO	0.192	0.013	0.039
MgO	14.11	9.10	9.92
CaO	11.80	11.80	11.87
Na_2O	1.762	1.361	1.483
K_2O	0.057	1.373	1.482
Total	96.42	96.51	97.23
Si	6.83	6.33	6.20
Ti	0.05	0.09	0.09
Al	1.75	2.61	2.75
Fe^{3+}	0.17	0.05	0.11
Fe^{2+}	1.14	1.89	1.68
Mn	0.02	0.002	0.005
Mg	3.06	2.05	2.20
Ca	1.84	1.90	1.89
Na	0.50	0.40	0.43
K	0.01	0.26	0.28
#Mg	0.73	0.52	0.57

from the GJAC main body were selected for Ar/Ar dating (Figure 2d). Representative analyses of the dated amphiboles are given in Table 1. Amphibolite sample GJ-9 is composed of magnesiohornblende (with Mg# = 0.60–0.73 and Si = 6.17–6.84 atoms per formula unit, apfu) and oligoclase (Xan = 0.41–0.43). Garnet amphibolite samples GJ-258a and GJ-259a are similar in terms of bulk-rock and mineral composition. Amphibole is pargasite/ferropargasite, with Mg# = 0.42–0.57. Garnet porphyroblasts are rich in almandine (Xalm = 0.44–0.48) and grossular (Xgrs = 0.41–0.47), and have low Mg# (0.10–0.15). Plagioclase has Xan = 0.26–0.50.

The bulk compositions of the dated samples are given in Table 2. These and all other analyses of amphibolites treated below were taken from Lázaro *et al.* (2013). Table 2 also shows two whole-rock analyses of serpentinites (GJ-3 and GJ-6) hosting amphibolitic layers.

Analytical methods

Amphibole composition was obtained by WDS with the CAMECA SX-50 microprobe of the University of Barcelona. The machine operated at 15 KeV and 15 nA with a beam size of 5 μm, and using mineral albite (Na), diposide (Si), wollastonite (Ca), vanadinite (Cl), sanidine (K), TiO_2 (Ti), rhodonite (Mn), $BaSO_4$ (Ba), CaF_2 (F), Fe_2O_3 (Fe), and synthetic periclase (Mg), Al_2O_3 (Al), Cr_2O_3 (Cr), NiO (Ni) as calibration standards. The composition of amphibole was normalized following the scheme of Leake *et al.* (1997), using the general formula $AB_2C_5T_8O_{22}(OH)_2$, and Fe^{3+} was estimated after the method of Schumacher (in Leake *et al.* (1997)).

For whole-rock analyses, the sample powders were prepared removing carefully secondary veins and Fe oxy-hydroxide/clay crust before sample crushing and powdering representative amounts of each sample in a tungsten carbide mill. Major element and Zr concentrations were determined on glass beads made up of ~0.6 g powdered sample diluted in 6 g of $Li_2B_4O_7$, by Philips Magix Pro (PW-2440) X Ray fluorescence (XRF) equipment at the University of Granada (Centro de Instrumentación Científica, CIC). Precision is better than ±1.5% for an analyte concentration of 10 wt.%. Precision for Zr and LOI is better than ±4% at 100 ppm concentration. Trace elements, except Zr, were determined at the University of Granada (CIC) by ICP Mass Spectrometry (ICP-MS) after HNO_3 + HF digestion of ~100 mg of sample powder in a Teflon-lined vessel at ~180°C and ~200 psi for 30 min, evaporation to dryness, and subsequent dissolution in 100 ml of 4 vol.% HNO_3. Procedural blanks and international standards PMS, WSE, UBN, BEN, BR, and AGV (Govindaraju 1994) were run as unknowns during analytical sessions. Precision was better than ±2% and ±5% for analyte concentrations of 50 and 5 ppm, respectively.

Hornblende crystals ranging in size from 150 to 200 μm were separated after crushing, sieving, and handpicking of single grains under a binocular microscope. The grains were repeatedly cleaned ultrasonically in distilled water. The selected crystals were co-irradiated for 30 h in the nuclear reactor at the McMaster University, Hamilton, Canada, in position 5c, along with a Fish Canyon Sanidine monitor (28.03 Ma ± 0.5%; Jourdan and Renne 2007). The total neutron flux density during irradiation was $8.8 \cdot 10^{18}$ n cm^{-2}, with a maximum flux gradient estimated at ±0.2% (1σ) in

Table 2. Major (wt%) and trace element (ppm) composition of serpentinites and dated Ar/Ar amphibolites from Güira de Jauco complex.

Petrological group	Common amphibolite	Garnet amphibolite		Serpentinite	
Sample	GJ9	GJ258a	GJ259a	GJ3	GJ6
GPS coordinates	−74º18′36.9″ 20º8′19.82″	−74º18′30.15″ 20º6′49.65″	−74º18′36.9″ 20º6′54.27″	74º18′29″ 20º7′22″	74º18′30.1″ 20º7′22.3″
SiO_2	51.0	49.6	50.5	42.4	40.2
TiO_2	1.76	1.42	1.29	0.040	0.041
Al_2O_3	13.2	19.5	19.0	1.65	1.39
Fe_2O_3tot	13.3	9.6	10.4	8.74	8.25
MnO	0.22	0.13	0.15	0.14	0.12
MgO	7.0	3.6	3.5	34.3	38.3
CaO	9.8	12.7	10.8	0.57	0.14
Na_2O	2.96	2.16	2.88	*n.a.*	0.018
K_2O	0.080	0.66	0.83	*n.a*	0.005
P_2O_5	0.085	0.15	0.14	0.011	0.005
LOI	0.52	0.31	0.37	11.8	12.6
Mg #	51.1	42.7	40.1	88.6	90.2
Zr (XRF)	66	96	79	6.2	6.1
Rb	1.86	9	15	0.63	0.15
Cs	0.008	1.05	0.21	0.0305	0.191
Be	0.63	0.67	0.75	0.1638	0.112
Sr	147	163	202	7.1	1.45
Ba	18.4	34	87	15.2	3.6
Sc	41	34	35	16.5	14.6
V	483	240	252	48	53
Cr	304	294	293	2422	2868
Co	47	59	52	104	109
Ni	69	107	83	1986	2187
Cu	10.5	82	51	11.9	19.1
Zn	119	86	90	40	52
Ga	17.1	18.0	17.6	2.0	1.512
Y	32	34	56	1.31	0.96
Nb	1.87	2.8	1.69	0.148	0.817
Ta	0.138	0.40	0.28	*b.d.l.*	2.3
Hf	0.69	1.02	0.84	*b.d.l.*	0.038
Mo	0.109	3.6	2.4	0.76	0.34
Sn	1.00	0.99	0.88	*b.d.l.*	*b.d.l.*
Tl	0	0	0	0.024	*b.d.l.*
Pb	0.63	0.40	0.48	1.20	0.152
U	0.35	0.23	0.23	0.051	0.007
Th	12.9	0.25	0.142	0.004	0.028
La	13.9	4.4	5.2	0.45	0.096
Ce	36	10.4	12.3	1.28	0.26
Pr	4.9	1.84	2.3	0.082	0.036
Nd	20	10.3	12.8	0.36	0.159
Sm	5.5	3.5	4.3	0.090	0.064
Eu	1.14	1.15	1.52	0.030	0.018
Gd	5.4	4.3	6.2	0.173	0.082
Tb	0.85	0.77	1.13	0.025	0.015
Dy	5.0	5.5	8.0	0.079	0.096
Ho	1.10	1.16	1.79	0.029	0.023
Er	2.9	3.3	5.0	0.129	0.064
Tm	0.45	0.51	0.74	0.019	0.010
Yb	2.8	3.0	4.8	0.190	0.079
Lu	0.41	0.46	0.75	0.018	0.013

Note: Mg# = 100*[(Mg/Fe^{2+}_{total} + Mg)atomic].

the volume where the samples were included. $^{40}Ar/^{39}Ar$ analyses of amphibole grains were performed at Geoazur Laboratory, University of Nice-Sophia Antipolis, France, by step-heating with a CO_2 Synrad laser. The gas was purified in a stainless and glass extraction line using two Al–Zr getters (working at 400°C and ambient temperature, respectively) and a liquid nitrogen cold trap. Isotopic measurements were performed with a VG3600 mass spectrometer

and a Daly-photomultiplier system. Blank measurements were obtained before and after every three-sample run. The correction factors for interfering isotopes correspond to $(^{39}Ar/^{37}Ar)_{Ca} = (7.30 \pm 0.28) \times 10^{-4}$; $(^{36}Ar/^{37}Ar)_{Ca} = (2.82 \pm 0.03) \times 10^{-4}$; and $(^{40}Ar/^{39}Ar)_{K} = (2.97 \pm 0.06) \times 10^{-2}$. Ages were calculated using the decay constants of Steiger and Jäger (1977) and the air $^{40}Ar/^{36}Ar$ ratio of 298.56 ± 0.31 (Lee *et al.* 2006). The criteria for defining plateau ages were as follows: (1) a plateau age should contain at least 70% of released ^{39}Ar; (2) there should be at least three successive steps in the plateau; and (3) the integrated age of the plateau should agree with each apparent age of the plateau within a 2σ error confidence interval.

Ar/Ar ages

The results of the $^{40}Ar/^{39}Ar$ incremental heating analyses and a summary of age and isochron calculation results are presented in Table 3 and are graphically shown in Figure 6. Hornblende of sample GJ-259a yielded a well-defined plateau age of 76.55 ± 2.03 Ma (2σ) based on 94.8 % of the released ^{39}Ar (steps 3, 4, 5, and 6; Table 3; Figure 6a). The normal isochron age is 78.57 ± 2.52 Ma and the inverse isochron age is 77.62 ± 1.78 Ma with a $^{40}Ar/^{36}Ar$ intercept at 188.1 ± 69.3 (Figure 6b). Hornblende of sample GJ-258a yielded a well-defined plateau age of 78.40 ± 1.88 Ma (2σ) based on 98.4% of the released ^{39}Ar (steps 2, 3, 4, and 5; Table 3; Figure 6c). The normal isochron age is 78.31 ± 1.84 Ma and the inverse isochron age is 78.40 ± 1.62 Ma with a $^{40}Ar/^{36}Ar$ intercept at 256.4 ± 71.0, which is close to the atmospheric value of 295.5 (Figure 6d). These two plateau ages overlap within error and are concordant. No plateau age was obtained on amphibole from sample GJ-9, which showed a pattern with slight variation and excess Ar in the first two steps and yielded an integrated age of 80.70 ± 7.58 Ma and a total fusion age of 82.85 ± 10.57 Ma (Figure 6e and f).

Discussion

Nature and geodynamic setting of the protoliths

Many sub-ophiolitic metamorphic soles worldwide are of MORB and/or OIB nature (e.g. Oman, Turkey, Syria; Al-Riyami *et al.* 2002; Dilek 2003; Ishikawa *et al.* 2005; Elitok and Drüppel 2008). However, several cases clearly show a supra-subduction origin and have been interpreted as resulting from subduction initiation within the supra-subduction zone (SSZ) lithosphere (e.g. Philippines, South Tibet, California; Encarnación (2004), Guilmette *et al.* (2009), and Wakabayashi *et al.* (2010)). Lázaro *et al.* (2013) characterized the protoliths of the GJAC amphibolites as N-MORB-like tholeiitic basalts formed in a back-arc setting based on bivariate major elements diagrams and N-MORB-, chondrite-normalized spider diagrams. Indeed, the slight enrichment in Th and La and depletion in Nb–Ta, Zr and Ti relative to N-MORB suggest melting of a supra-subduction zone mantle influenced by a subducting slab. This is shown in the multi-elemental diagrams (Figure 7), where the Güira de Jauco amphibolites

Table 3. $^{40}Ar/^{39}Ar$ analytical results.

Incremental heating		$^{36}Ar(a)$	$^{37}Ar(ca)$	$^{38}Ar(cl)$	$^{39}Ar(k)$	$^{40}Ar(r)$	Age ± 2σ (Ma)	$^{40}Ar(r)$ (%)	$^{39}Ar(k)$ (%)	K/Ca ± 2σ
Sample GJ-259a, amphibole, J = 0.00406330 ± 0.00004063										
K592–1	460.00 W	0.000121	0.000731	0.000014	0.000441	0.000539	8.93 ± 76.83	1.47	0.82	50.7 ± 11.5
K592–2	560.00 W	0.000057	0.008431	0.000000	0.002362	0.022476	68.43 ± 11.50	56.99	4.37	23.5 ± 1.6
K592–3	650.00 W	0.000031	0.032677	0.000000	0.009197	0.096294	75.16 ± 3.06	90.93	17.03	23.6 ± 1.6
K592–4	720.00 W	0.000019	0.056189	0.000000	0.014887	0.156946	75.67 ± 2.36	96.32	27.56	22.3 ± 1.4
K592–5	840.00 W	0.000004	0.016558	0.000000	0.004731	0.050878	77.15 ± 5.57	97.39	8.76	24.0 ± 1.6
K592–6	840.00 W	0.000012	0.091601	0.000000	0.022396	0.243161	77.88 ± 2.16	98.26	41.46	20.5 ± 1.3
Sample GJ-258a, amphibole, J = 0.00406650 ± 0.00004067										
K591–1	450.00 W	0.000029	0.000276	0.000000	0.000227	0.000973	31.14 ± 75.38	10.08	0.38	69.2 ± 38.9
K591–2	540.00 W	0.000017	0.030095	0.000000	0.008668	0.094100	77.94 ± 2.73	94.70	14.38	24.2 ± 1.6
K591–3	690.00 W	0.000008	0.063312	0.000000	0.017050	0.185448	78.08 ±1.96	98.51	28.28	22.6 ± 1.5
K591–4	825.00 W	−0.000012	0.051819	0.000000	0.013879	0.151419	78.31 ± 2.37	102.20	23.02	22.5 ± 1.5
K591–5	1111.00 W	−0.000016	0.079031	0.000000	0.020467	0.225244	78.98 ± 1.90	101.88	33.95	21.8 ± 1.4
Sample GJ-9, amphibole, J = 0.00406960 ± 0.00004070										
K590–1	460.00 W	0.000064	0.000256	0.000021	0.000020	0.002520	757.52 ± 1058.04	11.68	0.41	6.44 ± 6.62
K590–2	560.00 W	0.000027	0.006743	0.000091	0.000139	0.001470	75.95 ± 139.39	15.55	2.88	1.73 ± 0.18
K590–3	650.00 W	0.000042	0.134567	0.001133	0.002830	0.030283	76.91 ± 11.12	70.41	58.59	1.77 ± 0.12
K590–4	1111.00 W	0.000013	0.087259	0.000730	0.001841	0.021501	83.76 ± 9.96	84.10	38.12	1.77 ± 0.12

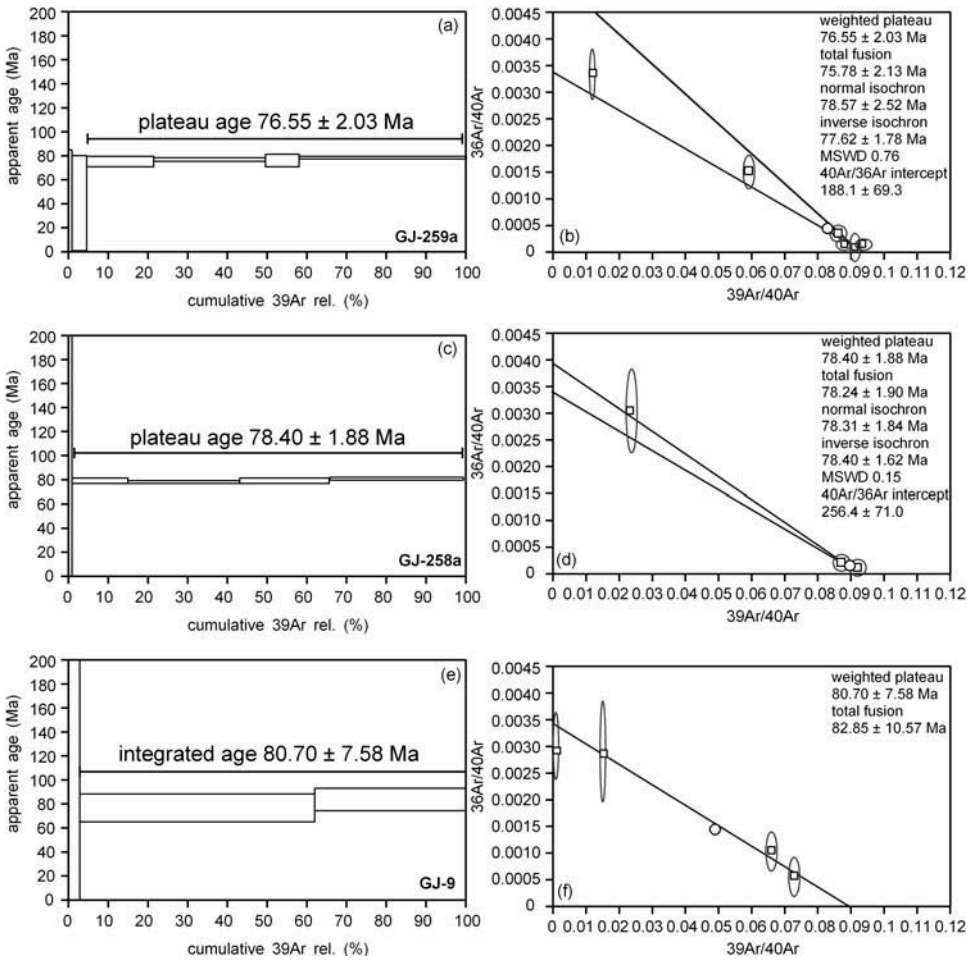

Figure 6. Incremental step-heating analyses of amphibole. The heights of the rectangles and all errors represent ±1σ uncertainty.

compare better to the samples of metamorphic soles with SSZ protholiths (Figure 7b).

Because of the likelihood of modification of major and some trace element compositions by sea-floor and subduction zone alteration processes, the use of the relatively immobile high-field strength elements (HFSEs: Nb, Ta, Zr, Hf), some large-ion lithophile elements (Th, light rare earth elements (LREEs): La, Ce, Nd), and the heavy rare earth elements (HREEs), and their ratios, is an useful tool in avoiding complications due to alteration of volcanic rocks (e.g. Pearce 2008). Ghatak *et al.* (2012) concluded that metabasalts from the Franciscan complex suffered subduction metamorphism that occurred in a largely closed system and, despite their metamorphism, these rocks preserve protolith major and trace elemental compositions and isotopic ratios, with the exception of some mobile large-ion lithophile elements such as Ba, Pb, and, to a lesser extent La, U, and Sr. The relations of the Th/Yb vs. Nb/Yb ratios consider less mobile elements in low-T aqueous fluids and hence are more convenient even in the study of altered and metamorphosed rocks (Pearce and Peate 1995; Pearce 2008). In this diagram (Figure 8a), the GJAC samples plot within and above the mantle array, suggesting a variable subduction component (Th can be transferred by hot fluids from the subducted sediments to the upper plate mantle; Pearce 2008). As expected, the Cretaceous volcanic arc complexes of the Téneme and Quibiján formations (IAT, Marchesi *et al.* 2007) plot in this diagram above the mantle array. The volcanics related to the Moa–Baracoa ophiolite (Morel, La Melba, and Centeno volcanics, group G1 in Figure 8) plot in the mantle array, overlapping the less enriched amphibolites. The dikes and micrograbbros intruding the Mayarí–Baracoa peridotites (Group G2 in Figure 8) define a vertical field from the mantle array towards enriched Th/Yb compositions as a function of the contribution of the subduction component. This field, in part, also overlaps with the studied amphibolites. These relations allow correlation of these eastern Cuba ophiolite-related basaltic rocks with the protoliths of the Güira de Jauco amphibolites, which also overlap with the field of the SSZ metamorphic soles from California and South Tibet

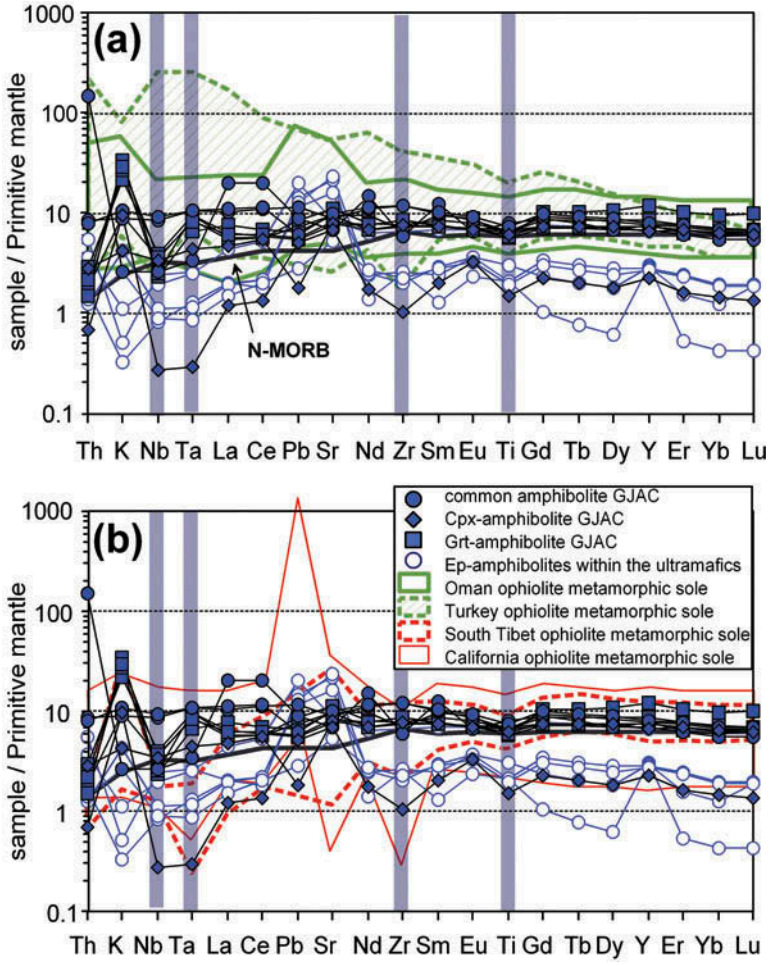

Figure 7. Trace element concentrations normalized over primitive mantle for amphibolites from GJAC and amphibolites within serpentinites compared to: (a) N-MORB and OIB protholiths of amphibolitic metamorphic soles from Oman and Turkey (Ishikawa *et al.* 2005; Elitok and Drüppel 2008); and (b) SSZ protholiths of amphibolitic metamorphic soles from South Tibet and California (Guilmette *et al.* 2009; Wakabayashi *et al.* 2010). N-MORB (Sun and McDonough 1989) is included for comparison.

(Figure 8a). Arc lavas have, in addition to Nb depletion and Th enrichment, high concentrations of Ba and Pb that, even if mobile, translate into relatively unperturbed high Ba/Pb, Ba/Th, Ba/Nb, U/Th, U/Nb, and La/Nb ratios (Wakabayashi *et al.* 2010). Figure 8b shows how the amphibolites from the GJAC display these signatures, exhibiting high Ba/Th ratios similar to eastern Cuba ophiolite-related basaltic rocks and other SSZ metamorphic sole protoliths.

The serpentinitic rocks that enclose layers of amphibolite are compared to other regionally related ultramafic complexes in Figure 9. These include the harzburgites of the Mayarí–Baracoa Ophiolite Belt (interpreted as highly refractory peridotites from an arc–back-arc environment; Marchesi *et al.* (2006)), serpentinites from the La Corea mélange (interpreted as accreted subducted abyssal metaperidotites; Blanco-Quintero *et al.* 2011b), the Monte del Estado complex in Puerto Rico (interpreted as obducted abyssal peridotite; Lewis *et al.* 2006; Marchesi *et al.* (2011)), Central Cuba serpentinites and Dominican Republic serpentinites from Camú and Septentrional fault zones (interpreted as fore-arc peridotites; Hattori and Guillot 2007; Saumur *et al.* 2010), and Dominican Republic peridotites from the Río San Juan subduction mélange and the Puerto Plata complex (interpreted as abyssal peridotites; Saumur *et al.* 2010). The serpentinite samples from the GJAC show compositions similar to the subducted abyssal peridotites from the La Corea serpentinitic mélange, the abyssal lherzolites of the Monte del Estado ultramafic complex, and the abyssal peridotites from Río San Juan and Puerto Plata complexes. The chondrite-normalized REE patterns of the serpentinites from the Güira de Jauco complex are relatively flat with slight variably enriched LREE (especially La and Ce; Figure 10). This pattern is similar to that of peridotites from the Monte del Estado complex and of worldwide

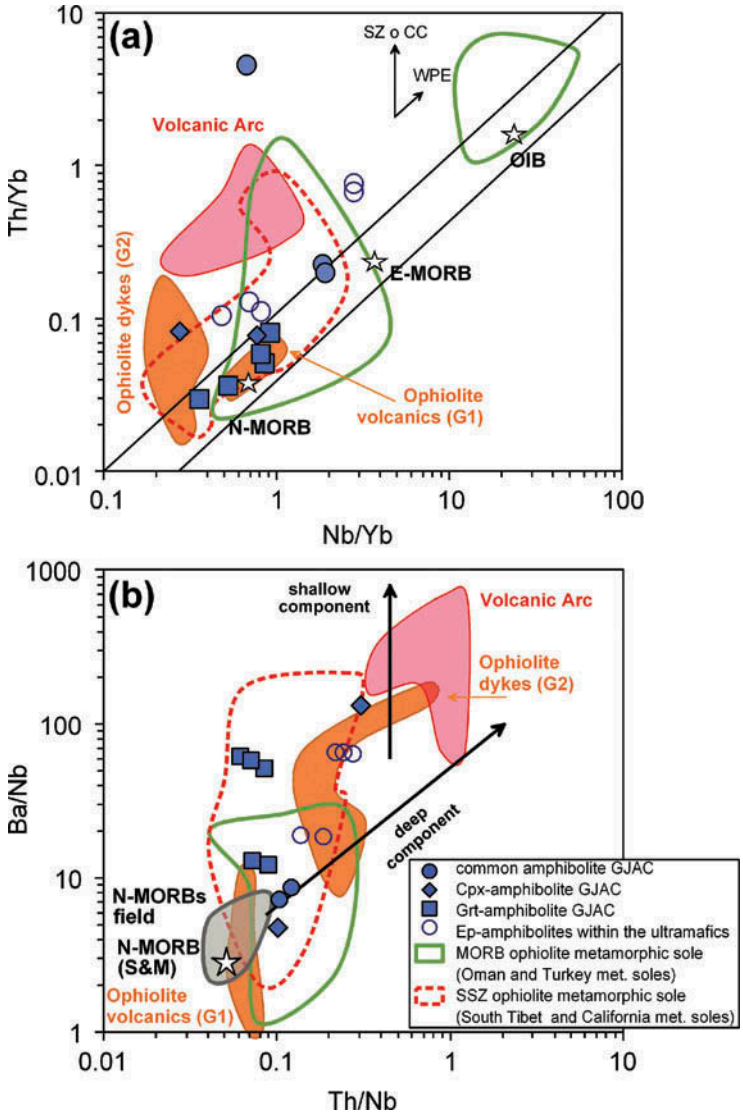

Figure 8. (a) Th/Yb *versus* Nb/Yb plot for the GJAC amphibolites. The Caribbean island arc is represented by the Cretaceous volcanic rocks of eastern Cuba (Téneme and Quibiján formations; Marchesi *et al.* 2007). The ophiolite-related basaltic rocks of Marchesi *et al.* (2007) include group G1 (Morel, La Melba, and Centeno formations) and group G2 (dikes and micrograbbros from Guamuta, Loma de la Bandera, and Cerrajón). Also shown are fields of MORB-OIB (Oman, Turkey,) and SSZ (South Tibet and California) protoliths of amphibolitic metamorphic soles (Ishikawa *et al.* 2005; Elitok and Drüppel 2008; Guilmette *et al.* 2009; Wakabayashi *et al.* 2010). N-MORB, E-MORB, and OIB values are from Sun and McDonough (1989). (b) Ba/Nb *versus* Th/Nb (Pearce and Stern 2006) proxy of depth of subduction components in back-arc basins. Ba/Nb is the proxy for total subduction input and Th/Nb the proxy for deep subduction input, so deep subduction gives a diagonal vector and shallow subduction gives a vertical vector. The diagram shows that amphibolites from the GJAC display influence of both components, similar to SSZ protholiths of amphibolitic metamorphic soles from South Tibet and California (Guilmette *et al.* 2009; Wakabayashi *et al.* 2010). The arc- and ophiolite-related basaltic rocks of eastern Cuba and N-MORB (star) as in (a). The field of N-MORB is from Pearce and Stern (2006).

subducted serpentinites (Deschamps *et al.* 2013). These authors consider that this type of REE pattern is the result of secondary enrichment, either magmatic at the site of formation of the peridotitic protoliths or, most importantly, metamorphic during hydration of the peridotites in the oceanic and the subduction realms. Hence, the chemical composition of the studied serpentinites compares well to enriched abyssal peridotites and enriched subducted abyssal or mantle wedge serpentinites but not to the refractory mantle wedge peridotites of the associated Moa–Baracoa (and Mayarí-Cristal) ophiolitic sheets.

Thus, geochemical features of the studied rocks offer the paradox that the amphibolites and ultramafic rocks of the GJAC are related and unrelated, respectively, to the basaltic and ultramafic rocks of the Moa–Baracoa ophiolite. This paradox can be resolved if both pieces of mantle

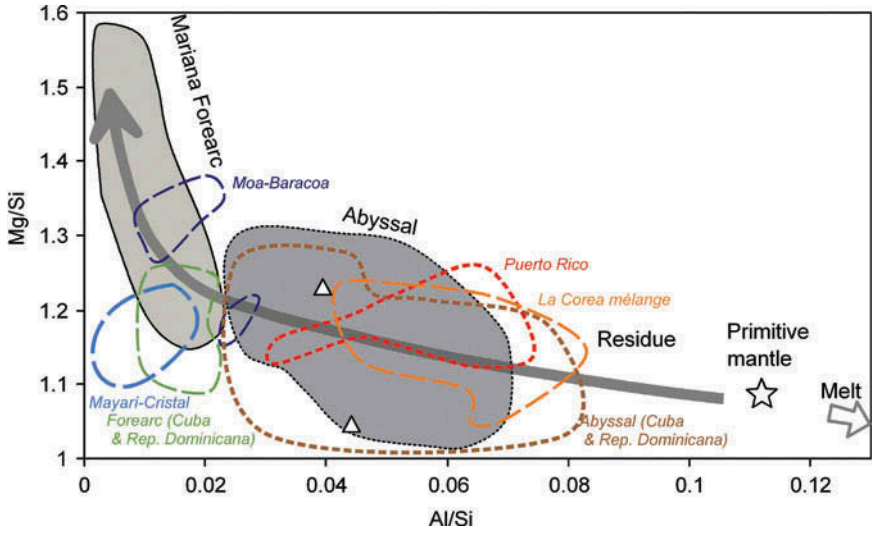

Figure 9. Weight ratios of Mg/Si *versus* Al/Si of serpentinite samples from the Güira de Jauco complex (white triangles). Plotted for comparison are the fields of Mayarí–Baracoa harzburgites (Marchesi *et al.* 2006), Monte del Estado peridotites (eastern Cuba; Marchesi *et al.* (2011)), abyssal serpentinites from the Dominican Republic (Saumur *et al.* 2010), subducted abyssal serpentinites from the La Corea mélange (eastern Cuba; Blanco-Quintero *et al.* (2011b)), and fore-arc serpentinites from Central Cuba and the Dominican Republic (Hattori and Guillot 2007; Saumur *et al.* 2010). Fields for Mariana fore-arc and abyssal peridotites compiled by Hattori and Guillot (2007). The primitive mantle value is from McDonough and Sun (1995).

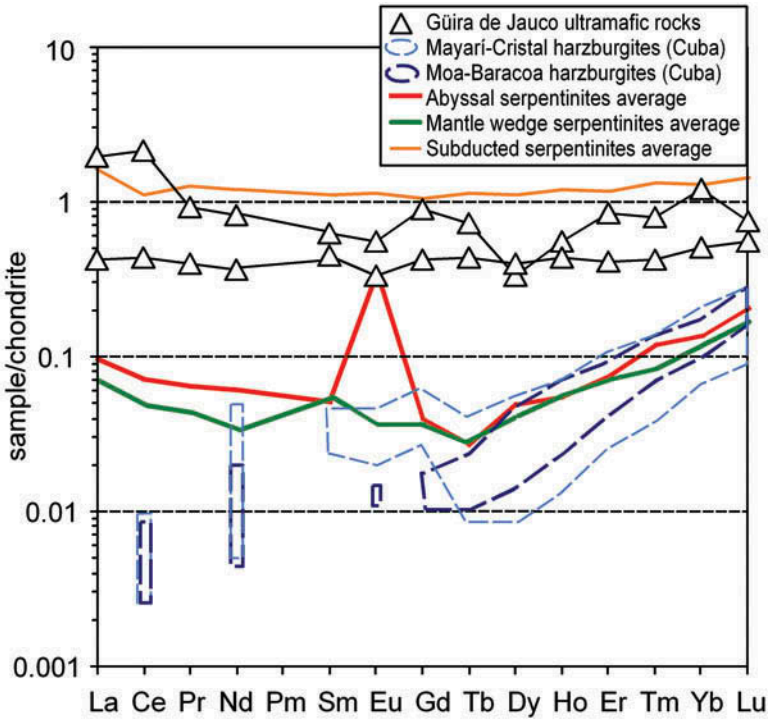

Figure 10. Chondrite (CI)-normalized (McDonough and Sun 1995) REE abundances of serpentinite samples from the Güira de Jauco complex. Plotted for comparison are the fields of Mayarí–Cristal and Moa–Baracoa harzburgites (eastern Cuba; Marchesi *et al.* (2006)). Also included are the average REE compositions of abyssal, mantle wedge, and subducted serpentinites derived from harzburgites compiled by Deschamps *et al.* (2013).

formed at different times and locations. Since the protoliths of the concordant amphibolite layers within the ultramafic rocks of the GJAC likely were emplaced as dikes intruding peridotites, what these ultramafic rocks probably represent is an older pre-intrusion back-arc oceanic basement, while the peridotites of the Moa–Baracoa ophiolite probably represent this same material that was later affected by intense melt extraction in the new fore-arc after subduction initiation in the back-arc. Alternatively, the peridotites of the Moa–Baracoa and Güira de Jauco complexes may represent the same mantle, but the latter suffered geochemical enrichment during serpentinization in the subduction environment (Deschamps *et al.* 2013).

Age of subduction initiation

Lázaro *et al.* (2013) calculated peak conditions of 658 ± 37°C, 8.6 ± 1.0 kbar, 662 ± 71°C, 8.7 ± 2.2 kbar, and 648 ± 51°C, 8.5 ± 1.7 kbar in samples of clinopyroxene- and garnet-bearing amphibolites (including the dated sample GJ-258a). These results suggest that most rocks underwent similar peak P-T conditions ranging from 648 to 665°C and 8.5 to 8.7 kbar, corresponding to an apparent geothermal gradient of ~20°C km^{-1}. This gradient is too high for mature subduction, but is consistent with an onset of subduction scenario, in agreement with general views of sub-ophiolitic metamorphic sole formation processes (Malpas 1979; Nicolas and Le Pichon 1980; Boudier *et al.* 1985, 1988; Hacker *et al.* 1996; Searle and Cox 2002; Wakabayashi and Dilek 2003; Robertson 2004; Stern 2004; Wakabayashi 2004; Agard *et al.* 2007; Cluzel *et al.* 2012).

The low-uncertainty hornblende $^{40}Ar/^{39}Ar$ mid-Campanian ages (76.55 ± 2.03 and 78.40 ± 1.88 Ma) represent cooling ages through the closure temperature for argon retention in amphibole (~500ºC; Harrison and FitzGerald 1986). The P-T paths of the amphibolites (Lázaro *et al.* 2013) indicate that cooling to approximately 500ºC took place at <15 km depth, during exhumation. On the other hand, the ~125 Ma zircon U–Pb age of a gabbroic dike from the Moa–Baracoa massif (Rojas-Agramonte *et al.* 2013) and the Turonian–Coniacian (palaeontological age; Iturralde-Vinent *et al.* 2006) age of the back-arc MORB-like Morel volcanics (Group G1 of Marchesi *et al.* (2007); Figure 2a) indicate that formation of the oceanic lithosphere in eastern Cuba endured for at least 35 Ma. This rather extended history of SSZ magmatism is also comparable to that recorded in the Trodoos ophiolite (Greece; Osozawa *et al.* (2012)). So, the metamorphic sole, GJAC, could have been formed only after this period of time. These time constraints allow exclusion of the subduction event represented by the subduction mélanges of La Corea and Sierra del Convento (eastern Cuba) and Río San Juan (Dominican Republic), which indicate subduction initiation by ca. 120 Ma or earlier (Krebs *et al.* 2008; Lázaro *et al.* 2009; Blanco-Quintero *et al.* 2010; 2011, 2011a; Cárdenas-Párraga *et al.* 2012; Escuder-Viruete *et al.* 2013).

A rapid sequence of onset of subduction and cooling/exhumation of the sole, consistent with evidence from other soles such as in Oman (e.g. Hacker 1990, 1994), would indicate that subduction initiation (and consequently peak metamorphic conditions) would occur shortly before 77–78 Ma (cooling to 500ºC), probably ca. 80–85 Ma. But slower-cooling evolution, such as in the Franciscan belt (Anczkiewicz *et al.* 2004) or the Sanbagawa belt, due to ridge approach (Japan; Aoya *et al.* 2003) is also possible. Moreover, the hypothesis of ridge subduction after subduction initiation has been proposed as a critical stage in the evolution of many SSZ ophiolites (Shervais 2001), especially in cases with long duration of SSZ magmatism (Osozawa *et al.* 2012). In the latter case, and using a cooling rate of 15ºC per million years (following Anczkiewicz *et al.* 2004), the metamorphic peak conditions would have been attained at ca. 90 Ma. Our data, however, do not allow constraining cooling rates and the timing of peak metamorphic conditions of the GJAC and, hence, as a compromise, we consider an age around 85 Ma for peak metamorphic conditions and onset of subduction.

Causes of subduction initiation

Geochronologic data (mostly Ar/Ar and nannofossils) suggest that volcanism of the CCOP began around 94 Ma in the eastern Pacific basin to the west of the volcanic arc of the Caribbean, and that the main pulse of plume activity occurred at 92–88 Ma but continued to 74 Ma and 63 Ma in the eastern Caribbean (Kerr *et al.* 2003; Loewen *et al.* 2013, and references therein). An Early-to-Late Cretaceous E-dipping subduction zone consuming Pacific lithosphere would have allowed the collision of the Pacific CCOP with the arc at ca. 85 Ma, causing a subduction polarity reversal (Figure 1d; Duncan and Hargraves 1984; Burke 1988; Kerr *et al.* 2003; Hastie *et al.* 2013). Hence, our data and inferences could be conceptualized within such a plateau–trench–arc collision and flip of subduction events at 85 Ma (Figure 1d and e). In this model, the new subduction zone would have started consuming Proto-Caribbean lithosphere by ca. 85 Ma, and the sole would have formed in a new fore-arc where the IAT volcanic arc rocks of Téneme and Quibiján(?) may have been formed. However, age data indicate that these IAT rocks formed earlier, at ca. 90 Ma (Proenza *et al.* 2006; Iturralde-Vinent *et al.* 2006), when the plateau was forming in the Farallon (Pacific) realm. In addition, other aspects of the regional geology of eastern Cuba can hardly be explained by this model (Figure 1e), as discussed below.

There is no evidence for the presence of the plateau in any geological element of eastern Cuba, as indicated by, for example, higher Nb, Nb/Y, and Zr/Y ratios in the

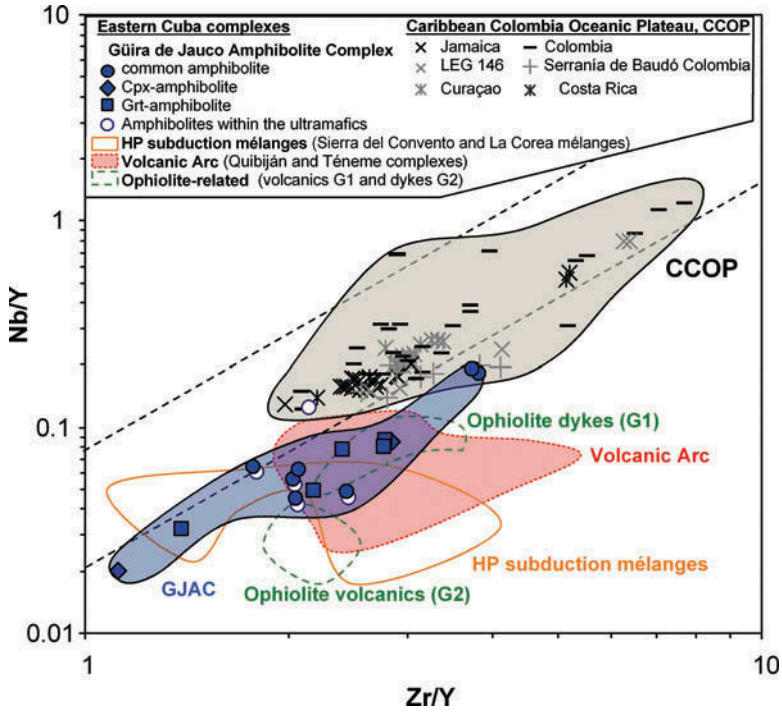

Figure 11. Nb/Y vs. Zr/Y diagram (Fitton *et al.* 1997) for eastern Cuba complexes, including the Güira de Jauco Amphibolite Complex (GJAC; geochemical data from Lázaro *et al.* 2013), volcanic arc and ophiolite complexes (Marchesi *et al.* 2006, 2007), and HP blocks of subduction mélanges (Lázaro and García-Casco 2008; Blanco-Quintero *et al.* 2010, 2011a). The Caribbean–Colombian Oceanic Plateau (CCOP) data are from Jamaica (Hastie *et al.* 2008), Colombia, LEG 146, Curaçao, Costa Rica (Nicoya and Quepos), and Serranía de Baudó Colombia (Hauff *et al.* 2000; Kerr *et al.* 2002).

plateau (cf. Fitton *et al.* 1997; Condie 1999; Figure 11), in agreement with the IAT, boninitic, and MORB-like signatures and formation in supra-subduction environments of eastern Cuba ophiolites. On the other hand, there is geochemical evidence for the involvement of North America-derived sediments in the genesis of the eastern Cuban ophiolitic volcanics (Marchesi *et al.* 2007), including the protoliths of the GJAC and the related Morel formation (Lázaro *et al.* 2013). These data imply SW subduction of the Proto-Caribbean Ocean beneath the Caribbean plate since at least 91 Ma (Iturralde-Vinent *et al.* 2006), when the plateau was in its initial stages of formation. Furthermore, subduction and blueschist facies metamorphism of the Cretaceous volcanic arc Purial complex during the Late Cretaceous (70–75 Ma; Somin *et al.* 1992; García-Casco *et al.* 2006; Iturralde-Vinent *et al.* 2006; 2008a) is not predicted by E-directed Pacific subduction followed by post-85 Ma W-directed Proto-Caribbean subduction (Figure 1d and e). Finally, Early-to-Late Cretaceous ages of high-pressure metamorphic rocks of eastern Cuba and Río San Juan (Dominican Republic) support models of SW-dipping subduction beneath the Greater Antilles Arc since at least the Aptian (García-Casco *et al.* 2006; Pindell *et al.* 2006; Krebs *et al.* 2008, 2011; Lázaro *et al.* 2009, 2011; Blanco-Quintero *et al.* 2011a; Escuder-Viruete *et al.* 2013). This is in agreement with recent tomographic models that image the detached Proto-Caribbean slab from 800 km (updip end) down to 1200–1500 km (downdip end) in the lower mantle, implying a length of subducted oceanic lithosphere before the Eocene (when the slab detached and the Lesser Antilles slab started to subduct) ranging 800–2100 km (as a function of slab thickening factor; van Benthem *et al.* 2013). Van Benthem *et al.* (2013) concluded that these figures are in agreement with plate reconstructions that suggest subduction of the Proto-Caribbean/Atlantic in the mid-Cretaceous (e.g. Meschede and Frisch 1998; Pindell and Kennan 2009), and van der Meer *et al.* (2010) agreed that the age of the base of the slab is 118–110 Ma or older following García-Casco *et al.* (2002, 2008a, 2008b); Krebs *et al.* (2008); Lázaro *et al.* (2009); Blanco-Quintero *et al.* (2011a); Harlow *et al.* (2004); and Brueckner *et al.* (2009). Thus, even if the Caribbean plateau collided/subducted with/below the Caribbean arc during the Late Cretaceous in Jamaica (West *et al.* 2014), we conclude that the model that better accounts for the tectonic/petrologic development of eastern Cuba is one in which such subduction polarity reversal at 85 Ma is not involved (Figures 1c, d, and 12).

In our model for eastern Cuba, the general NE vergence of the structures (e.g. Cobiella *et al.* 1984; Nuñez Cambra *et al.* 2004) affecting the ophiolites, the high-

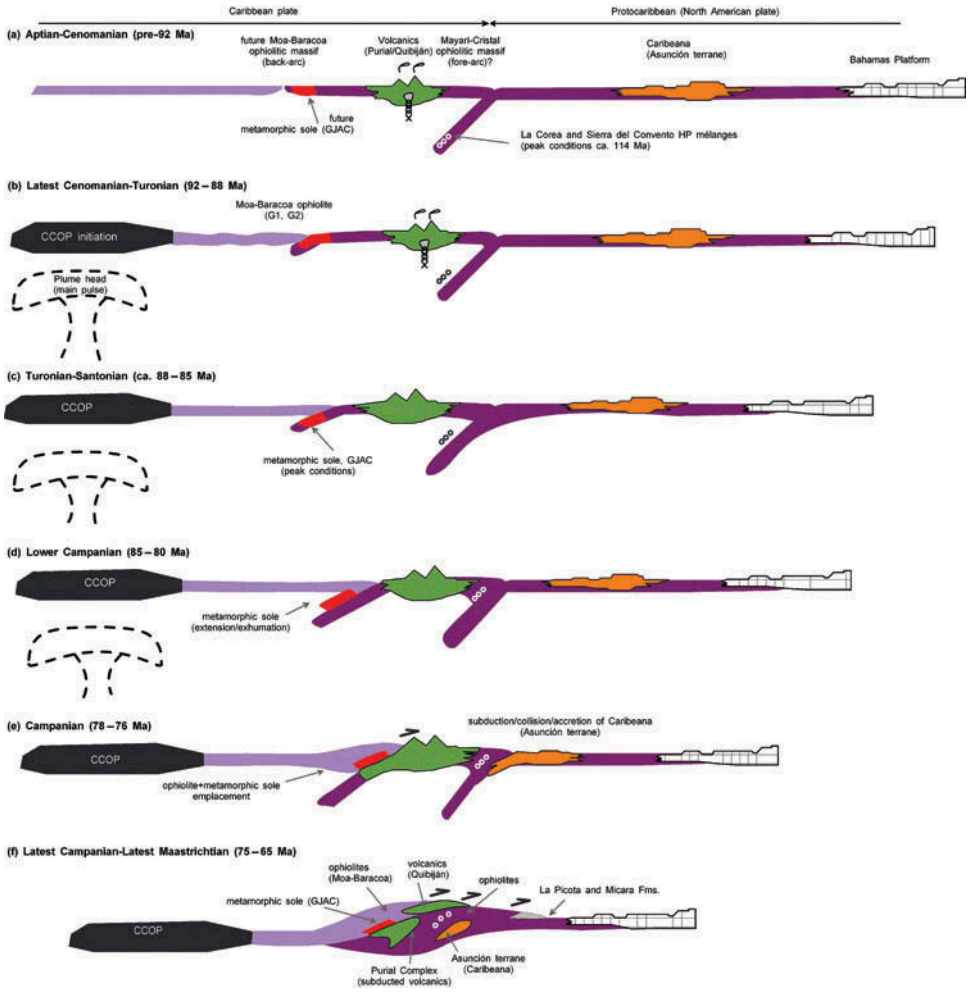

Figure 12. Tectonic configuration and evolution of eastern Cuba in Cretaceous times with the proposed setting of the metamorphic complex of Güira de Jauco and other complexes mentioned in the text.

pressure rocks of El Purial and Asunción complexes, and the Cretaceous volcanic arc complexes is related to a sequence of collisions triggered by two W-dipping subduction zones (Figure 12; García-Casco *et al.* 2006; Lázaro *et al.* 2013). In this model (Figure 12a), the Moa–Baracoa ophiolite evolved from at least 125 Ma (Rojas-Agramonte *et al.* 2013) to ca. 90 Ma (Iturralde-Vinent *et al.* 2006), when it was in a back-arc setting (Marchesi *et al.* 2007). A new W-dipping subduction zone developed near the back-arc ridge in the range 90–85 Ma, forming the metamorphic sole at approximately 30 km depth in a relatively high thermal gradient due to subduction of hot young lithosphere into a hot upper plate mantle environment (Figure 12b and c). This process simultaneously formed a fore-arc arc in the new convergent margin where the Moa–Baracoa ophiolite evolved, in agreement with common views of the nature and evolution of fore-arcs (Gerya 2011; Whattam and Stern 2011; Stern *et al.* 2012, and references therein; Figure 12b and c). This stage was followed by subduction/collision of the Caribbean volcanic arc (metavolcanic Purial complex) in the new subduction zone at ca. 75 Ma, shortly before the Asunción terrane (i.e. Caribeana) subducted at ~75–70 Ma (Figure 12e and f; García-Casco *et al.* 2006, 2008a; Lázaro *et al.* 2009) in the older subduction zone of the Proto-Caribbean. Both subduction/accretion processes involving buoyant arc and continental margin-like crust triggered NE-directed ophiolite emplacement, collision, and synorogenic basin development (70–65 Ma; Figure 12f; Iturralde-Vinent *et al.* 2006).

Obduction of ophiolites over a continental margin or an arc, and the process of subduction inception, have been related to plume pulse events (e.g. Vaughan and Scarrow 2003; Dilek and Ernst 2008; Dilek and Furnes 2011). Indeed, the fact that the main pulse of the CCOP is almost co-etaneous with the inferred Late Cretaceous onset of the subduction event in eastern Cuba suggests a causal relationship. Many authors have pointed out the mechanical

difficulty in emplacing dense oceanic lithosphere over less dense rocks (e.g. Wakabayashi and Dilek 2003; Stern 2004; and references therein). Agard *et al.* (2007) proposed a mechanism that helps solve the density problem. In their model, these authors suggested that the two recent large global-scale events of ophiolite obduction (Upper Jurassic and Upper Cretaceous) coincide with periods in which plate convergence velocities increased, even doubled, in response to plume events. In their model, subduction initiation would be triggered by plate acceleration and instability caused by plume pulses. This mechanical hypothesis finds support in the close time relation between the main Jurassic and Cretaceous episodes of ophiolite obduction and superplume events all over the world (Vaughan and Scarrow 2003; Dilek and Ernst 2008; Dilek and Furnes 2011). Other mechanical models also relate plume (e.g. Burov and Cloetingh 2010) or oceanic plateau (e.g. Nair and Chacko 2008) influence on subduction initiation, with subduction dip towards the plume/plateau, as proposed here (Figure 12). Hence, the tectonic perturbation of the Caribbean–Colombian plume in the Caribbean plate can be envisaged as a hypothesis to account for the continuous sequence of events described here, including subduction inception towards the plateau, sole formation, closure of a back-arc basin, subduction of the Caribbean volcanic arc, and obduction of ophiolites above the arc (Figure 12). This model, however, does not exclude regional tectonic complications such as local or regional subduction of the Farallon/Caribbean lithosphere below the Caribbean arc since the mid or Late Cretaceous in a manner similar to the present-day Muertos or South Caribbean subduction zones (Figure 1a; Pindell and Kennan 2009; Miller *et al.* 2009; van Benthem *et al.* 2013 and references therein) that may account for particular structures or petrologic bodies such as the Mt Hibernia Schist of Jamaica that document subduction of the CCOP after ca. 90 Ma (West *et al.* 2014).

Conclusions

This study is complementary to the preliminary geochemical study presented in Lázaro *et al.* (2013). The geochemical approach based on immobile elements allows one to conclude that the protoliths of the Moa–Baracoa metamorphic sole (the Güira de Jauco Amphibolite Complex) formed in a SSZ environment, probably in a back-arc basin, that contrasts with other MORB/OIB soles elsewhere. The geochemical similarity among the amphibolites and the basic rocks from the overlying non-metamorphosed ophiolite suggests that they might have a similar origin and protolith. We offer here the first Ar–Ar data obtained for these rocks, which precisely indicate metamorphic cooling ages of 76.5–78.5 Ma during initial exhumation of the sole. An age of ca. 85 Ma is suggested for peak metamorphism and related onset of subduction. The rapid sequence of events involving the main Caribbean–Colombian plume pulse (92–88 Ma) and the processes of sole formation and subduction initiation (85 Ma) suggest a causal relation in which the activity of the plume triggered local plate acceleration and onset of subduction with subduction dip towards the plateau/plume. The new data and geological considerations support a model in which the inception of a new subduction (Late Cretaceous) occurred at the back-arc of the early-Late Cretaceous Caribbean arc related to subduction of the Proto-Caribbean (Atlantic) lithosphere, shortly before arc–continent collision (75 Ma–Eocene) took place at the northern leading edge of the Caribbean plate.

Acknowledgements

This is a contribution to IGCP-546 'Subduction zones of the Caribbean'. We are grateful to J. Wakayabashi and an anonymous reviewer for their careful revision of an earlier version of this manuscript.

Funding

We appreciate financial support from Spanish MINECO projects CGL2009-12446 and CGL2012-36263.

References

Agard, P., Jolivet, L., Vrielynck, B., Burov, E., and Monié, P., 2007, Plate acceleration: The obduction trigger?: Earth and Planetary Science Letters, v. 258, p. 428–441. doi:10.1016/j.epsl.2007.04.002

Al-Riyami, K., Robertson, A., Dixon, J.E., and Xenophontos, C., 2002, Origin and emplacement of the Late Cretaceous Baer–Bassit ophiolite and its metamorphic sole in NW Syria: Lithos, v. 65, p. 225–260. doi:10.1016/S0024-4937(02)00167-6

Anczkiewicz, R., Platt, J.P., Thirlwall, M.F., and Wakabayashi, J., 2004, Franciscan subduction off to a slow start: Evidence from high-precision Lu–-Hf garnet ages on high grade-blocks: Earth and Planetary Science Letters, v. 225, p. 147–161. doi:10.1016/j.epsl.2004.06.003

Anderson, T.H., Erdlac, R.J., and Sandstrom, M.A., 1985, Late-Cretaceous allochthons and post-Cretaceous strike-slip displacement along the Cuilco-Chixoy-Polochic Fault, Guatemala: Tectonics, v. 4, p. 453–475. doi:10.1029/TC004i005p00453

Aoya, M., Uehara, S., Matsumoto, M., Wallis, S.R., and Enami, M., 2003, Subduction-stage pressure-temperature path of eclogite from the Sambagawa belt: Prophetic record for oceanic-ridge subduction: *Geology*, v. 31, p. 1045–1048. doi:10.1130/G19927.1

Blanco-Quintero, I.F., Garcia-Casco, A., Rojas-Agramonte, Y., Rodriguez-Vega, A., Lazaro, C., and Iturralde-Vinent, M.A., 2010, Metamorphic evolution of subducted hot oceanic crust (La Corea Melange, Cuba): American Journal of Science, v. 310, p. 889–915. doi:10.2475/11.2010.01

Blanco-Quintero, I.F., Proenza, J.A., García-Casco, A., Tauler, E., and Galí, S., 2011b, Serpentinites and serpentinites within a fossil subduction channel: La Corea mélange, eastern Cuba: Geologica Acta, v. 9, no. 3–4, p. 389–405.

Blanco-Quintero, I.F., Rojas-Agramonte, Y., García-Casco, A., Kröner, A., Mertz, D.F., Lázaro, C., Blanco-Moreno, J., and Renne, P.R., 2011a, Timing of subduction and exhumation in a subduction channel: evidence from slab melts from La Corea mélange (eastern Cuba): Lithos, v. 127, p. 86–100. doi:10.1016/j.lithos.2011.08.009

Boiteau, A., Michard, A., and Saliot, P., 1972, Métamorphisme de Haute Pression dans le Complexe Ophiolitique du Purial (Oriente, Cuba): Centre National Recherche Scientiphique, v. 274, p. 2137–2140.

Boudier, F., Bouchez, J.L., Nicolas, A., Cannat, M., Ceuleneer, G., Misseri, M., and Montigny, R., 1985, Kinematics of oceanic thrusting in the Oman ophiolite: Model of plate convergence: Earth and Planetary Science Letters, v. 75, p. 215–222. doi:10.1016/0012-821X(85)90103-7

Boudier, F., Ceuleneer, G., and Nicolas, A., 1988, Shear zones, thrusts and related magmatism in the Oman ophiolite: Initiation of thrusting on an oceanic ridge: Tectonophysics, v. 151, p. 275–296. doi:10.1016/0040-1951(88)90249-1

Brueckner, H.K., Avé Lallemant, H.G., Sisson, V.B., Harlow, G.E., Hemming, S.R., Martens, U., Tsujimori, T., and Sorensen, S.S., 2009, Metamorphic reworking of a high pressure–low temperature mélange along the Motagua fault, Guatemala: A record of Neocomian and Maastrichtian transpressional tectonics: Earth and Planetary Science Letters, v. 284, p. 228–235. doi:10.1016/j.epsl.2009.04.032

Burke, K., 1988, Tectonic evolution of the Caribbean: Annual Review of Earth and Planetary Sciences, v. 16, p. 201–230. doi:10.1146/annurev.ea.16.050188.001221

Burov, E., and Cloetingh, S., 2010, Plume-like upper mantle instabilities drive subduction initiation: Geophysical Research Letters, v. 37, p. L03309. doi:10.1029/2009GL041535

Cárdenas-Párraga, J., García-Casco, A., Harlow, G.E., Blanco-Quintero, I.F., Rojas-Agramonte, Y., and Kröner, A., 2012, Hydrothermal origin and age of jadeitites from Sierra del Convento Mélange (Eastern Cuba): European Journal of Mineralogy, v. 24, p. 313–331. doi:10.1127/0935-1221/2012/0024-2171

Cluzel, D., Jourdan, F., Meffre, S., Maurizot, P., and Lesimple, S., 2012, The metamorphic sole of New Caledonia ophiolite: 40Ar/ 39Ar, U–Pb, and geochemical evidence for subduction inception at a spreading ridge: Tectonics, v. 31, p. TC3016. doi:10.1029/2011TC003085

Cobiella, J., 1974, Los Macizos Serpentiníticos de Sabanilla, Mayarí Arriba: Oriente: Revistatecnológica, v. 12, no. 4, p. 41–50.

Cobiella, J., Quintas, F., Campos, M., and Hernández, M., 1984, Geología de la Región Central y Suroriental de la Provincia de Guantánamo: Santiago de Cuba, 125 p, Oriente, Santiago de Cuba.

Cobiella-Reguera, J.L., 2005, Emplacement of Cuban ophiolites: Geological Acta, v. 3, p. 273–294.

Condie, K.C., 1999, Mafic crustal xenoliths and the origin of the lower continental crust: Lithos, v. 46, p. 95–101. doi:10.1016/S0024-4937(98)00056-5

De Zoeten, R., and Mann, P., 1999, Cenozoic El Mamey Group of northern Hispaniola: A sedimentary record of subduction, collisional and strike-slip events within the North America-Caribbean Plate Boundary Zone, *in* Mann, P., ed., Caribbean basins: Sedimentary basins of the world: Ámsterdam, Elsevier, p. 247–286.

Deschamps, F., Godard, M., Guillot, S., and Hattori, K., 2013, Geochemistry of subduction zone serpentinites: A review: Lithos, v. 178, p. 96–127. doi:10.1016/j.lithos.2013.05.019

Dilek, Y., 2003, Ophiolite concept and its evolution, *in* Dilek, Y., and Newcomb, S., eds., Ophiolite concept and the evolution of geological thought: Geological Society of America, Special Papers, v. 373, p. 1–16.

Dilek, Y., and Ernst, R., 2008, Links between ophiolites and Large Igneous Provinces (LIPs) in Earth history: Introduction: Lithos, v. 100, p. 1–13. doi:10.1016/j.lithos.2007.08.001

Dilek, Y., and Furnes, H., 2011, Ophiolite genesis and global tectonics: Geochemical and tectonic fingerprinting of ancient oceanic lithosphere: Geological Society of America Bulletin, v. 123, p. 387–411. doi:10.1130/B30446.1

Duncan, R.A., and Hargraves, R.B., 1984, Plate tectonic evolution of the Caribbean region in the mantle reference frame, *in* Bonini, W.E., Hargraves, R.B., and Shagam, R., eds., The Caribbean-South American plate boundary and regional tectonics: Geological Society of America, Memoirs 162, p. 81–94. doi:10.1130/MEM162-p81

Elitok, Ö., and Drüppel, K., 2008, Geochemistry and tectonic significance of metamorphic sole rocks beneath the Beyşehir–Hoyran ophiolite (SW-Turkey): Lithos, v. 100, p. 322–353. doi:10.1016/j.lithos.2007.06.022

Encarnación, J., 2004, Multiple ophiolite generation preserved in the northern Philippines and the growth of an island arc complex: Tectonophysics, v. 392, p. 103–130. doi:10.1016/j.tecto.2004.04.010

Escuder-Viruete, J., Pérez-Estaún, A., Gabites, J., and Suárez-Rodríguez, Á., 2011, Structural development of a high-pressure collisional accretionary wedge: The Samaná complex, northern Hispaniola: Journal of Structural Geology, v. 33, p. 928–950. doi:10.1016/j.jsg.2011.02.006

Escuder-Viruete, J., Valverde-Vaquero, P., Rojas-Agramonte, Y., Gabites, J., Castillo-Carrión, M., and Pérez-Estaún, A., 2013, Timing of deformational events in the Río San Juan complex: Implications for the tectonic controls on the exhumation of high-P rocks in the northern Caribbean subduction-accretionary prism: Lithos, v. 177, p. 416–435. doi:10.1016/j.lithos.2013.07.006

Fitton, J.G., Saunders, A.D., Norry, M.J., Hardarson, B.S., and Taylor, R.N., 1997, Thermal and chemical structure of the Iceland plume: Earth and Planetary Science Letters, v. 153, p. 197–208. doi:10.1016/S0012-821X(97)00170-2

Garcia-Casco, A., 2007, Magmatic paragonite in trondhjemites from the Sierra del Convento melange, Cuba: American Mineralogist, v. 92, p. 1232–1237. doi:10.2138/am.2007.2598

García-Casco, A., Iturralde-Vinent, M.A., and Pindell, J., 2008a, Latest Cretaceous collision/ accretion between the Caribbean Plate and Caribeana: Origin of metamorphic terranes in the Greater Antilles: International Geology Review, v. 50, p. 781–809. doi:10.2747/0020-6814.50.9.781

Garcia-Casco, A., Lazaro, C., Rojas-Agramonte, Y., Kroner, A., Torres-Roldan, R.L., Nunez, K., Neubauer, F., Millan, G., and Blanco-Quintero, I., 2008b, Partial melting and counterclockwise P T path of subducted oceanic crust (Sierra del Convento Melange, Cuba): Journal of Petrology, v. 49, p. 129–161. doi:10.1093/petrology/egm074

García-Casco, A., Rodríguez Vega, A., Cárdenas Párraga, J., Iturralde-Vinent, M.A., Lázaro, C., Blanco Quintero, I., Rojas-Agramonte, Y., Kröner, A., Núñez Cambra, K., Millán, G., Torres-Roldán, R.L., and Carrasquilla, S., 2009, A new jadeitite jade locality (Sierra del Convento, Cuba): First report and some petrological and archeological implications: Contributions to Mineralogy and Petrology, v. 158, p. 1–16. doi:10.1007/s00410-008-0367-0

García-Casco, A., Torres-Roldán, R.L., Iturralde-Vinent, M.A., Millán, G., Núñez Cambra, K., Lázaro, C., and Rodríguez Vega, A., 2006, High pressure metamorphism of ophiolites in Cuba: Geologica Acta, v. 4, p. 63–88.

Garcia-Casco, A., Torres-Roldan, R.L., Millan, G., Monie, P., and Schneider, J., 2002, Oscillatory zoning in eclogitic garnet and amphibole, northern serpentinite melange, Cuba: A record of tectonic instability during subduction?: Journal of Metamorphic Geology, v. 20, p. 581–598. doi:10.1046/j.1525-1314.2002.00390.x

Gerya, T.V., 2011, Intra-oceanic subduction zones, *in* Brown, D., and Ryan, P.D., eds., Arc-continent collision, frontiers in earth sciences: Berlin, Heidelberg, Springer-Verlag, p. 23–51. doi:10.1007/978-3-540-88558-0_2

Ghatak, A., Basu, A.R., and Wakabayashi, J., 2012, Elemental mobility in subduction metamorphism: Insight from metamorphic rocks of the Franciscan Complex and the Feather River ultramafic belt, California: International Geology Review, v. 54, p. 654–685. doi:10.1080/00206814.2011.567087

Govindaraju, K., 1994, Compilation of working values and sample description for 383 geostandards: Geostandards and Geoanalytical Research, v. 18, p. 1–158. doi:10.1111/j.1751-908X.1994.tb00502.x

Guilmette, C., Hébert, R., Wang, C.S., and Villeneuve, M., 2009, Geochemistry and Geochronology of the metamorphic sole underlying the Xigaze Ophiolite, Yarlung Zangbo Suture Zone, South Tibet: Lithos, v. 112, p. 149–162. doi:10.1016/j.lithos.2009.05.027

Gyarmati, P., 1983, Las formaciones metamórficas de Cuba oriental, *in* Alvear, J.F., Nagy, E., and Radócz, G., eds., Contribución a la Geología de Cuba Oriental: La Habana, Cuba, Editorial Científico-Técnica, p. 90–98.

Gyarmati, P., Méndez, I., and Lay, M., 1997, Caracterización de las rocas del arco de islas Cretácico en la Zona Estructuro-Facial Nipe-Cristal-Baracoa, *in* Furrazola, G.F., and Nuñez-Cambra, K.E., eds., Estudios sobre Geología de Cuba: Ciudad de la Habana, Cuba, Instituto de Geología y Paleontología, p. 357–364.

Hacker, B.R., 1990, Simulation of the metamorphic and deformational history of the metamorphic sole of the Oman ophiolite: Journal of Geophysical Research, v. 95, p. 4895–4907. doi:10.1029/JB095iB04p04895

Hacker, B.R., 1994, Rapid emplacement of young oceanic lithosphere: Argon geochronology of the Oman ophiolite: Science, v. 265, p. 1563–1565. doi:10.1126/science.265.5178.1563

Hacker, B.R., Mosenfelder, J.L., and Gnos, E., 1996, Rapid emplacement of the Oman ophiolite: Thermal and geochronologic constraints: Tectonics, v. 15, p. 1230–1247. doi:10.1029/96TC01973

Harlow, G.E., Hemming, S.R., Avé Lallemant, H.G., Sisson, V. B., and Sorensen, S.S., 2004, Two high-pressure–low-temperature serpentinite-matrix mélange belts, Motagua fault zone, Guatemala: A record of Aptian and Maastrichtian collisions: Geology, v. 32, p. 17–20. doi:10.1130/G19990.1

Harrison, T.M., and FitzGerald, J.D., 1986, Exsolution in hornblende and its consequences for age spectra and closure temperature: Geochimica Et Cosmochimica Acta, v. 50, p. 247–253. doi:10.1016/0016-7037(86)90173-0

Hastie, A.R., and Kerr, A.C., 2010, Mantle plume or slab window?: Physical and geochemical constraints on the origin of the Caribbean oceanic plateau: Earth-Science Reviews, v. 98, p. 283–293. doi:10.1016/j.earscirev.2009.11.001

Hastie, A.R., Kerr, A.C., Mitchell, S.F., and Millar, I.L., 2008, Geochemistry and petrogenesis of Cretaceous oceanic plateau lavas in eastern Jamaica: Lithos, v. 101, p. 323–343. doi:10.1016/j.lithos.2007.08.003

Hastie, A.R., Mitchell, S.F., Treloar, P.J., Kerr, A.C., Neill, I., and Barfod, D.N., 2013, Geochemical components in a Cretaceous island arc: The Th/La–(Ce/Ce*)Nd diagram and implications for subduction initiation in the inter-American region: Lithos, v. 162-163, p. 57–69. doi:10.1016/j.lithos.2012.12.001

Hattori, K.H., and Guillot, S., 2007, Geochemical character of serpentinites associated with high- to ultrahigh-pressure metamorphic rocks in the Alps, Cuba, and the Himalayas: Recycling of elements in subduction zones: Geochemistry, Geophysics, Geosystems, v. 8, p. Q09010. doi:10.1029/2007GC001594

Hauff, F., Hoernle, K., Tilton, G., Graham, D.W., and Kerr, A.C., 2000, Large volume recycling of oceanic lithosphere over short time scales: Geochemical constraints from the Caribbean Large Igneous Province: Earth and Planetary Science Letters, v. 174, p. 247–263. doi:10.1016/S0012-821X(99)00272-1

Ishikawa, T., Fujisawa, S., Nagaishi, K., and Masuda, T., 2005, Trace element characteristics of the fluid liberated from amphibolite-facies slab: Inference from the metamorphic sole beneath the Oman ophiolite and implication for boninite genesis: Earth and Planetary Science Letters, v. 240, p. 355–377. doi:10.1016/j.epsl.2005.09.049

Iturralde-Vinent, M., 1976, Estratigrafía de la Zona Calabazas-Achotal, Mayarí Arriba, Oriente: Revista La Minería En Cuba, v. 1, no. 5, p. 9–23.

Iturralde-Vinent, M., 1996a, Geología de las ofiolitas de Cuba, *in* Iturralde-Vinent, M., ed., Ofiolitas y arcos volcánicos de Cuba: Miami, USA, IGCP Project 364, p. 83–120.

Iturralde-Vinent, M., 1996b, Cuba: el arco de islas volcánicas del Cretácico, *in* Iturralde-Vinent, M., ed., Ofiolitas y arcos volcánicos de Cuba: Miami, FL, IGCP Project 364, p. 179–189.

Iturralde-Vinent, M.A., 1998, Sinopsis de la Constitución Geológica de Cuba: Acta Geológica Hispánica, v. 33, p. 9–56.

Iturralde-Vinent, M.A., Díaz Otero, C., Garcia-Casco, A., and Van Hinsbergen, D., 2008, Paleogene Foredeep Basin deposits of North-Central Cuba: A record of Arc-Continent collision between the Caribbean and North American Plates: International Geology Review, v. 50, p. 863–884. doi:10.2747/0020-6814.50.10.863

Iturralde-Vinent, M.A., Díaz-Otero, C., Rodríguez-Vega, A., and Díaz-Martínez, R., 2006, Tectonic implications of paleontologic dating of Cretaceous-Danian sections of Eastern Cuba: Geologica Acta, v. 4, p. 89–102.

Jourdan, F., and Renne, P.R., 2007, Age calibration of the Fish Canyon sanidine 40Ar/39Ar dating standard using primary K-Ar standards: Geochimica Et Cosmochimica Acta, v. 71, p. 387–402. doi:10.1016/j.gca.2006.09.002

Kerr, A.C., Iturralde-Vinent, M., Saunders, A.D., Babbs, T.L., and Tarney, J., 1999, A new plate tectonic model of the Caribbean: Implications from a geochemical reconnaissance of Cuban Mesozoic volcanic rocks: Geological Society of America Bulletin, v. 111, p. 1581–1599. doi:10.1130/0016-7606(1999)111<1581:ANPTMO>2.3.CO;2

Kerr, A.C., Tarney, J., Kempton, P.D., Spadea, P., Nivia, A., Marriner, G.F., and Duncan, R.A., 2002, Pervasive mantle plume head heterogeneity: Evidence from the late Cretaceous Caribbean-Colombian Oceanic Plateau: Journal of Geophysical Research, v. 107, no. B7, p. ECV 2-1–ECV 2-13. doi:10.1029/2001JB000790

Kerr, A.C., White, R.V., Thompson, P.M.E., Tarney, J., and Saunders, A.D., 2003, No oceanic plateau—no Caribbean

plate? The seminal role of an oceanic plateau in Caribbean plate evolution, *in* Bartolini, C., Buffler, R.T., and Blickwede, J., eds., The Circum Gulf of Mexico and Caribbean: Hydrocarbon Habitats basin formation and plate tectonics: American Association of Petroleum Geologist Memoirs 79, p. 126–268.

Knipper, A.L., and Cabrera, R., 1974, Téctonica y geología histórica de la zona de articulación entre el mio- y eugeosinclinal y del cinturón hiperbasítico de Cuba: Academia de Ciencias de Cuba, Instituto de Geología, Contribución a la geología de Cuba, p. 15–77.

Krebs, M., Maresch, W.V., Schertl, H.-P., Münker, C., Baumann, A., Draper, G., Idleman, B., and Trapp, E., 2008, The dynamics of intra-oceanic subduction zones: A direct comparison between fossil petrological evidence (Rio San Juan Complex, Dominican Republic) and numerical simulation: Lithos, v. 103, p. 106–137. doi:10.1016/j.lithos.2007.09.003

Krebs, M., Schertl, H.P., Maresch, W.V., and Draper, G., 2011, Mass flow in serpentinite-hosted subduction channels: P–T–t path patterns of metamorphic blocks in the Rio San Juan mélange (Dominican Republic): Journal of Asian Earth Sciences, v. 42, p. 569–595. doi:10.1016/j.jseaes.2011.01.011

Lázaro, C., Blanco-Quintero, I.F., Rojas-Agramonte, Y., Proenza, J.A., Núñez-Cambra, K., and García-Casco, A., 2013, First description of a metamorphic sole related to ophiolite obduction in the northern Caribbean: Geochemistry and petrology of the Güira de Jauco Amphibolite Complex (eastern Cuba) and tectonic implications: Lithos, v. 179, p. 193–210. doi:10.1016/j.lithos.2013.08.019

Lázaro, C., and García-Casco, A., 2008, Geochemical and Sr–Nd isotope signatures of pristine slab melts and their residues (Sierra del Convento mélange, eastern Cuba): Chemical Geology, v. 255, p. 120–133. doi:10.1016/j.chemgeo.2008.06.017

Lázaro, C., García-Casco, A., Rojas Agramonte, Y., Kröner, A., Neubauer, F., and Iturralde-Vinent, M., 2009, Fifty-five million-year history of oceanic subduction and exhumation at the northern edge of the Caribbean plate (Sierra del Convento mélange, Cuba): Journal of Metamorphic Geology, v. 27, p. 19–40. doi:10.1111/j.1525-1314.2008.00800.x

Leake, B.E., Woolley, A.R., Arps, C.E.S., Birch, W.D., Gilbert, M.C., Grice, J.D., Hawthorne, F.C., Kato, A., Kisch, H.J., Krivovichev, V.G., Linthout, K., Laird, J., Mandarino, J.A., Maresch, W.V., Nickel, E.H., Rock, N.M.S., Schumacher, J. C., Smith, D.C., Stephenson, N.C.N., Ungaretti, L., Whittaker, E.J.W., and Youzhi, G., 1997, Nomenclature of amphiboles: Report of the Subcommittee on Amphiboles of the International Mineralogical Association, Commission on New Minerals and Mineral Names: American Mineralogist, v. 82, p. 1019–1037.

Lee, J.Y., Marti, K., Severinghaus, J.P., Kawamura, K., Yoo, H. S., Lee, J.B., and Kim, J.S., 2006, A redetermination of the isotopic abundances of atmospheric Ar: Geochimica Et Cosmochimica Acta, v. 70, p. 4507–4512. doi:10.1016/j.gca.2006.06.1563

Lewis, G.E., and Straczek, J.A., 1955, Geology of South-Central Oriente Province, Cuba: US Geological Survey Bulletin, v. 975-D, p. 171–336.

Lewis, J.F., Draper, G., Proenza, J.A., Espaillat, J., and Jimenez, J., 2006, Ophiolite-related ultramafic rocks (Serpentinites) in the Caribbean region: A review of their occurrence, composition, origin, emplacement and nickel laterite soils: Geologica Acta, v. 4, p. 237–263.

Loewen, M.W., Duncan, R.A., Kent, A.J.R., and Kyle Krawl, K., 2013, Prolonged plume volcanism in the Caribbean Large Igneous Province: New insights from Curaçao and Haiti: Geochemistry, Geophysics, Geosystems, v. 14. doi:10.1002/ggge.20273

Malpas, J., 1979, The dynamothermal aureole of the Bay of Islands ophiolite suite: Canadian Journal of Earth Sciences, v. 16, p. 2086–2101. doi:10.1139/e79-198

Marchesi, C., Garrido, C.J., Bosch, D., Proenza, J.A., Gervilla, F., Monie, P., and Rodriguez-Vega, A., 2007, Geochemistry of Cretaceous magmatism in eastern Cuba: Recycling of North American continental sediments and implications for subduction polarity in the Greater Antilles Paleo-arc: Journal of Petrology, v. 48, p. 1813–1840. doi:10.1093/petrology/egm040

Marchesi, C., Garrido, C.J., Godard, M., Proenza, J.A., Gervilla, F., and Blanco-Moreno, J., 2006, Petrogenesis of highly depleted peridotites and gabbroic rocks from the Mayarí-Baracoa Ophiolitic Belt (eastern Cuba): Contributions to Mineralogy and Petrology, v. 151, p. 717–736. doi:10.1007/s00410-006-0089-0

Marchesi, C., Jolly, W.T., Lewis, J.F., Garrido, C.J., Proenza, J.A., and Lidiak, E.G., 2011, Petrogenesis of fertile mantle peridotites from the Monte del Estado massif (Southwest Puerto Rico): A preserved section of Proto-Caribbean lithospheric mantle?: Geologica Acta, v. 9, p. 289–306.

McDonough, W.F., and Sun, S.S., 1995, The composition of the Earth: Chemical Geology, v. 120, p. 223–253. doi:10.1016/0009-2541(94)00140-4

Meschede, M., and Frisch, W., 1998, A plate-tectonic model for the Mesozoic and Early Cenozoic history of the Caribbean plate: Tectonophysics, v. 296, p. 269–291. doi:10.1016/S0040-1951(98)00157-7

Millán, G., 1996, Metavulcanitas del Purial, *in* Iturralde-Vinent, M., ed., Cuban ophiolites and volcanic arcs: Miami, IGCP Project 364 Special Contribution, 1, p. 218–221.

Millán, G., 1997, Posición estratigráfica de las metamorfitas cubanas, *in* Furrazola Bermúdez, G.F., and Núñez Cambra, K.E., eds., Estudios sobre Geología de Cuba: La Habana, Cuba, Centro Nacional de Información Geológica, p. 251–258.

Millán, G., and Somin, M.L., 1985, Contribución al conocimiento geológico de las metamorfitas del Escambray y Purial: Reporte De Investigación De La Academia De Ciencias De Cuba, v. 2, p. 1–74.

Millan, G., Somin, M.L., and Diaz, C., 1985, Nuevos datos sobre la geología del macizo montañoso de la Sierra del Purial, Cuba Oriental. Instituto de Geología y Paleontología, La Habana, Cuba: Reporte De Investigación No, v. 2, p. 52–74.

Miller, M.S., Levander, A., Niu, F., and Li, A., 2009, Upper mantle structure beneath the Caribbean-South American plate boundary from surface wave tomography: Journal of Geophysical Research, v. 114, p. B01312. doi:10.1029/2007JB005507

Nair, R., and Chacko, T., 2008, Role of oceanic plateaus in the initiation of subduction and origin of continental crust: Geology, v. 36, p. 583–586. doi:10.1130/G24773A.1

Nicolas, A., and Le Pichon, X., 1980, Thrusting of young lithosphere in subduction zones with special reference to structures in ophiolitic peridotites: Earth and Planetary Science Letters, v. 46, p. 397–406. doi:10.1016/0012-821X(80)90053-9

Nuñez Cambra, K.E., García-Casco, A., Iturralde-Vinent, M.A., and Millán, G., 2004, Emplacement of the ophiolite complex in Eastern Cuba, *in* 32nd International Geological Congress,

Session G20.11 Caribbean Plate Tectonics: Florencia, Proceedings, CD-rom.

Osozawa, S., Shinjo, R., Lo, C.-H., Jahn, B., Hoang, N., Sasaki, M., Ishikawa, K., Kano, H., Hoshi, H., Xenophontos, C., and Wakabayashi, J., 2012, Geochemistry and geochronology of the Troodos ophiolite: An SSZ ophiolite generated by subduction initiation and an extended episode of ridge subduction?: Lithosphere, v. 4, p. 497–510. doi:10.1130/L205.1

Pearce, J.A., 2008, Geochemical fingerprinting of oceanic basalts with applications to ophiolite classification and the search for Archean oceanic crust: Lithos, v. 100, p. 14–48. doi:10.1016/j.lithos.2007.06.016

Pearce, J.A., and Peate, D.W., 1995, Tectonic implications of the composition of volcanic arc magmas: Annual Review of Earth and Planetary Sciences, v. 23, p. 251–285. doi:10.1146/annurev.ea.23.050195.001343

Pearce, J.A., and Stern, R.J., 2006, The origin of back-arc basin magmas: Trace element and isotopic perspectives, *in* Christie, D.M., Fisher, C.R., Lee, S.-M., and Givens, S., eds, Back-arc spreading systems: Geological, biological, chemical, and physical interactions: Washington, DC, AGU monograph 166, p. 63–86.

Pindell, J., and Kennan, L., 2009, Tectonic evolution of the Gulf of Mexico, Caribbean and northern South America in the mantle reference frame: An update, *in* James, K.H., Lorente, M.A., and Pindell, J.L., eds., The origin and evolution of the Caribbean plate: London, Geological Society, Special Publications 328, p. 1–55.

Pindell, J.L., and Draper, G., 1991, Geologic development of the Puerto Plata region, northern Dominican Republic, *in* Mann, P., Draper, G., and Lewis, J.F., eds., Geological and tectonic development of the North American-Caribbean plate boundary in Hispaniola: Geological Society of America Special Paper 262, p. 97–114.

Pindell, J.L., Kennan, L., Maresch, W.V., Stanek, K.P., Draper, G., and Higgs, R., 2005, Plate kinematics and crystal dynamics of circum- Caribbean arc-continent interactions: Tectonic controls on basin development in Proto-Caribbean margins, *in* Avé Lallemant, H.G., and Sisson, V.B., eds., Caribbean-South American plate interactions, Venezuela: Geological Society of America Special Paper 394, p. 7–52.

Pindell, J.L., Kennan, L., Stanek, K.P., Maresch, W.V., and Draper, G., 2006, Foundations of Gulf of Mexico and Caribbean evolution: Eight controversies resolved: Geologica Acta, v. 4, p. 89–128.

Pindell, J.L., Maresch, W.V., Martens, U., and Stanek, K.P., 2012, The Greater Antillean Arc: Early Cretaceous origin and proposed relationship to Central American subduction mélanges: Implications for models of Caribbean evolution: International Geology Review, v. 54, p. 131–143. doi:10.1080/00206814.2010.510008

Proenza, J., Gervilla, F., Melgarejo, J.C., and Bodinier, J.L., 1999, Al- and Cr-rich chromitites from the Mayari-Baracoa ophiolitic belt (eastern Cuba); consequence of interaction between volatile-rich melts and peridotites in suprasubduction mantle: Economic Geology, v. 94, p. 547–566. doi:10.2113/gsecongeo.94.4.547

Proenza, J.A., Díaz-Martínez, R., Iriondo, A., Marchesi, C., Melgarejo, J.C., Gervilla, F., Garrido, C.J., Rodríguez-Vega, A., Lozano-Santacruz, R., and Blanco-Moreno, J.A., 2006, Primitive island-arc Cretaceous volcanic rocks in eastern Cuba: The Téneme Formation: Geologica Acta, v. 4, p. 103–121.

Pushcharovsky, Y., ed., 1988, Mapa geológico de la República de Cuba escala 1:250 000: Academias de Ciencias de Cuba y la URSS.

Quintas, F., 1987, Formación Mícara en Yumurí Arriba, Baracoa, clave para la interpretación de la Geología Histórica Pre-Paleocénica de Cuba Oriental: Revista Geología Y Minería, v. 5, no. 3, p. 3–20.

Quintas, F., 1988, Características estratigráficas y estructurales del complejo ofiolítico y eugeosinclinal de la cuenca del Río Quibiján, Baracoa: Minería Y Geología, v. 6, p. 11–22.

Quintas, F., 1989, Análisis estratigráfico y paleogeografía del Cretácico superior y del Paleógeno de la provincia de Guantánamo y áreas cercanas [Doctoral thesis]: Holguín, Cuba, Instituto Superior Minero Metalúrgico de Moa., 161 p.

Robertson, A., 2004, Development of concepts concerning the genesis and emplacement of Tethyan ophiolites in the Eastern Mediterranean and Oman regions: Earth Science Reviews, v. 66, p. 331–387. doi:10.1016/j.earscirev.2004.01.005

Rojas-Agramonte, Y., García-Casco, A., Kröner, A., and Kemp, T., 2013, On the origin of Precambrian to Triassic zircon grains from the Cuban juvenile intra-oceanic arc formations and ophiolitic complexes: International Meeting on Precambrian Evolution and Deep Exploration of the Continental Lithosphere, Beijing, China.

Rojas-Agramonte, Y., Neubauer, F., Bojar, A.V., Hejl, E., Handler, R., and García-Delgado, D.E., 2006, Geology, age and tectonic evolution of the Sierra Maestra Mountains, southeastern Cuba: Geologica Acta, v. 4, p. 123–150.

Saumur, B.-M., Hattori, K.H., and Guillot, S., 2010, Contrasting origins of serpentinites in a subduction complex, northern Dominican Republic: Geological Society of America Bulletin, v. 122, p. 292–304. doi:10.1130/B26530.1

Searle, M.P., and Cox, J., 2002, Subduction zone metamorphism during formation and emplacement of the Semail ophiolite in the Oman Mountains: Geological Magazine. doi:10.1017/S0016756802006532

Shervais, J.W., 2001, Birth, death, and resurrection: The life cycle of supra subduction zone ophiolites: Geochemistry, Geophysics, Geosystems, v. 2, no. 1. doi:10.1029/2000GC000080

Sinton, C.W., Duncan, R.A., Storey, M., Lewis, J., and Estrada, J. J., 1998, An oceanic flood basalt province within the Caribbean plate: Earth and Planetary Science Letters, v. 155, p. 221–235. doi:10.1016/S0012-821X(97)00214-8

Solari, L.A., Garcia-Casco, A., Martens, U., Lee, J.K.W., and Ortega-Rivera, A., 2013, Late Cretaceous subduction of the continental basement of the Maya block (Rabinal granite, central Guatemala): Tectonic implications for the geodynamic evolution of Central America: Geological Society of America Bulletin, v. 125, p. 625–639. doi:10.1130/B30743.1

Somin, M., and Millán, G., 1972, The metamorphic complexes of Pinos, Escambray and Oriente in Cuba and its ages (in Russian): Izvestia Akad Nauk SSSR, Geology, v. 5, p. 48–57.

Somin, M.L., Arakelyants, M.M., and Kolesnikov, E.M., 1992, Age and tectonic significance of high-pressure metamorphic rocks of Cuba: International Geology Review, v. 34, p. 105–118. doi:10.1080/00206819209465587

Somin, M.L., and Millán, G., 1981, Geology of the metamorphic complexes of Cuba (in Russian): Nauka, Moscow, p. 218.

Steiger, R.H., and Jäger, E., 1977, Subcommission on geochronology: convention on the use of decay constants in geo- and cosmochronology: Earth and Planetary Science Letters, v. 36, p. 359–362. doi:10.1016/0012-821X(77)90060-7

Stern, R.J., 2004, Subduction initiation: Spontaneous and induced: Earth and Planetary Science Letters, v. 226, p. 275–292. doi:10.1016/j.epsl.2004.08.007

Stern, R.J., Reagan, M., Ishizuka, O., Ohara, Y., and Whattam, S., 2012, To understand subduction initiation, study forearc crust: To understand forearc crust, study ophiolites: Lithosphere, v. 4, p. 469–483. doi:10.1130/L183.1

Sun, S.S., and McDonough, W.F., 1989, Chemical and isotope systematics of oceanic basalts: Implications for mantle composition and processes, *in* Saunders, A.D., and Norry, M.J., eds., Magmatism in ocean basins: Geological Society of London Special Publication 42, p. 313–345.

Torrez, M., and Fonseca, E., 1990, Características geológicas petrológicas del contacto entre la asociación ofiolítica y el arco volcánico en Moa-Baracoa: Boletín De Geociencias, Centro Universitario De Pinar Del Río, Cuba, v. 1, p. 12–19.

van Benthem, S., Govers, R., Spakman, W., and Wortel, R., 2013, Tectonic evolution and mantle structure of the Caribbean: Journal of Geophysical Research: Solid Earth, v. 118, p. 3019–3036. doi:10.1002/jgrb.50235

van der Meer, D.G., Spakman, W., van Hinsbergen, D.J.J., Amaru, M.L., and Torsvik, T.H., 2010, Towards absolute plate motions constrained by lower-mantle slab remnants: Nature Geoscience, v. 3, p. 36–40. doi:10.1038/ngeo708

Vaughan, A.P. M., and Scarrow, J.H., 2003, Ophiolite obduction pulses as a proxy indicator of superplume events?: Earth and Planetary Science Letters, v. 213, p. 407–416. doi:10.1016/S0012-821X(03)00330-3

Wakabayashi, J., 2004, Tectonic mechanisms associated with P–T paths of regional metamorphism: Alternatives to single-cycle thrusting and heating: Tectonophysics, v. 392, p. 193–218. doi:10.1016/j.tecto.2004.04.012

Wakabayashi, J., and Dilek, Y., 2003, What constitutes "emplacement" of an ophiolite?: Mechanisms and relationship to subduction initiation and formation of metamorphic soles, *in* Dilek, Y., and Robinson, P.T., eds., Ophiolites and Earth history: Geological Society London Special Publication 218, p. 427–448.

Wakabayashi, J., Ghatak, A., and Basu, A.R., 2010, Suprasubduction-zone ophiolite generation, emplacement, and initiation of subduction: A perspective from geochemistry, metamorphism, geochronology, and regional geology: Geological Society of America Bulletin, v. 122, p. 1548–1568. doi:10.1130/B30017.1

West Jr., D.P., Abbott, R.N., Bandy, B.R., and Kunk, M.J., 2014, Protolith provenance and thermotectonic history of metamorphic rocks in eastern Jamaica: Evolution of a transform plate boundary: Geological Society of America Bulletin, v. 126, no. 3–4, p. 600–614. doi:10.1130/B30704.1

Whattam, S.A., and Stern, R.J., 2011, The 'subduction initiation rule': A key for linking ophiolites, intra-oceanic forearcs, and subduction initiation: Contributions to Mineralogy and Petrology, v. 162, p. 1031–1045. doi:10.1007/s00410-011-0638-z